Communications Biology

https://doi.org/10.1038/s42003-026-09952-w

Article in Press

Genomic insights into antimicrobial resistance in ocular pathogens from India

Received: 26 June 2025

Accepted: 18 March 2026

Cite this article as: Kumar, V.S., Pandiyan, A., Bhagat, R. *et al.* Genomic insights into antimicrobial resistance in ocular pathogens from India. *Commun Biol* (2026). https://doi.org/10.1038/s42003-026-09952-w

Vanitha Shyamili Kumar, Apuratha Pandiyan, Rakeshpal Bhagat, Arvind Kumar, Reuben Jacob Mathew, Sreenivas Ara, Ankita Ramdas Punde, Likhita Laveti, Aruna Panda, Bhupesh Bagga, Vinay Kumar Nandicoori, Prashant Garg, Divya Tej Sowpati, Joveeta Joseph & Karthik Bharadwaj Tallapaka

Genomic Insights into Antimicrobial Resistance in Ocular Pathogens from India

Vanitha Shyamili Kumar[a,#], Apuratha Pandiyan[a,#], Rakeshpal Bhagat[a], Arvind Kumar[a,b], Reuben Jacob Mathew[a], Sreenivas Ara[a], Ankita Ramdas Punde[a], Likhita Laveti[c], Aruna Panda[a], Bhupesh Bagga[c], Vinay Kumar Nandicoori[a,b,d], Prashant Garg[c], Divya Tej Sowpati[a,b,*], Joveeta Joseph[c,*], Karthik Bharadwaj Tallapaka[a,b,*]

a Centre for Cellular and Molecular Biology, Hyderabad, India

b Academy of Scientific and Innovative Research (AcSIR), Ghaziabad, India

c Brien Holden Eye Research Centre, Hyderabad Eye Research Foundation, LV Prasad Eye Institute, Hyderabad, India

d National Institute of Immunology, New Delhi, India

# Equal contribution

* Corresponding authors

Address for correspondence

Dr Karthik Bharadwaj Tallapaka
CSIR - Centre for Cellular & Molecular Biology,
Habsiguda, Uppal Road, Hyderabad, Telangana,
India - 500 007
Phone: +9140 2719 2613

E-mail addresses for correspondence: karthikt.ccmb@csir.res.in; tej@ccmb.res.in; joveeta@lvpei.org

Abstract

Ocular infections have a substantial impact on global visual health. Despite their association with severe vision impairment, very few studies have systematically monitored antimicrobial resistance (AMR) over time using whole genome sequencing approaches. In the current study, we assembled 291 high fidelity bacterial genomes isolated from patients attending a tertiary eye care centre in India, using long-read sequencing. *Pseudomonas aeruginosa* (n = 62) and *Staphylococcus aureus* (n = 60) were the most common pathogens in the cohort, with more than 45% of isolates exhibiting multidrug resistance and more than 15% classified as extensively drug-resistant. Genotype–phenotype analyses and multilocus sequence typing revealed a previously unreported *mecA*-negative methicillin-resistant *Staphylococcus aureus* strain, ST9578, resistant to vancomycin and teicoplanin. Potential AMR mechanisms like a mutation in the 23S rRNA gene associated with linezolid resistance and a KorB-like protein encoding gene associated with fluoroquinolone resistance were identified using comparative genomics. This is the first large-scale genomic surveillance effort focused on ocular pathogens in the Indian subcontinent and the potential AMR mechanisms and sequence types identified underscores the need for larger such studies in low-and-middle-income countries.

Keywords

ocular infection, genomic surveillance, WGS, ONT, AMR, XDR *K. pneumoniae*, ST395, ST231, ARGs, NDM, ESBL, plasmids, HGT, LMIC, 23S ribosomal RNA, Linezolid resistance

Introduction

Antimicrobial resistance (AMR) contributes to 8-9% of all global deaths due to infectious causes, with the highest burden seen in low-and middle-income countries (LMICs)[1]. It is estimated that the AMR burden could result in 10 million deaths annually by 2050[2,3]. In ocular infections, AMR leads to ocular morbidity and vision loss due to prolonged therapy, reliance on antibiotics with severe side effects, increased risk of surgical interventions, and higher chances of therapeutic failure[4,5]. *Pseudomonas aeruginosa* (*P. aeruginosa)*, *Staphylococcus aureus* (*S. aureus)* and *Streptococcus pneumoniae* are among the commonly implicated pathogens in ocular infections[6,7]. These pathogens demonstrate differing rates of AMR in different regions of the world. For example, *P. aeruginosa* isolates from ocular infections in the USA were largely multidrug-susceptible, whereas isolates from India show significantly higher multidrug resistance (MDR) rates[6–9] with nearly half of the bacterial strains exhibiting MDR and increasing trends of resistance to fluoroquinolones and cephalosporins[10,11].

Though studies like Antibiotic Resistance Monitoring in Ocular Microorganisms (ARMOR) have tried to understand the AMR patterns in organisms causing ocular infections longitudinally, the impact of AMR on ocular infections has been under-reported globally[12]. Few recently published studies attempted to address this lacuna. An eight-year retrospective study from India reported increasing resistance to fluoroquinolones and cefoxitin in gram-negative isolates, and to fluoroquinolones, macrolides, and tetracyclines in gram-positive isolates from conjunctival swabs[13]. A Chinese study found high resistance rates to quinolones, aminoglycosides, and β-lactams among gram-positive bacteria, particularly in *Staphylococcus* species[14]. A four-year surveillance study from Turkey reported susceptibility of S. epidermidis to topical fluoroquinolones[15] and aminoglycosides, but high methicillin resistance. An Italian study demonstrated good activity to fluoroquinolones and glycopeptides against gram-positive isolates, consistent with the findings from Turkish study, but reported emerging resistance to aminoglycosides, third-generation cephalosporins and amoxicillin among gram-negative isolates[16]. The ARMOR study reports high rates of MDR among staphylococci. However, resistance rates to various antibiotics remained largely stable during the study period in the USA[17]. These studies reflect region specific trends in antibiotic resistance in ocular infections and underscore the need for region specific surveillance programs.

To combat the growing resistance, several global action plans have been introduced by AMR committees and collaborators, aiming to address infection prevention and reduction of the AMR

burden[18-20]. In 2022, a series of workshops conducted by the Surveillance and Epidemiology of Drug-resistant Infections Consortium (SEDRIC) strongly recommended integrating genomics into routine AMR surveillance in healthcare facilities[21,22]. This approach holds significant promise to strengthen infection prevention efforts and advance disease management practices[19,22,23]. Therefore, to understand the genomic signatures involved in AMR in ocular infections, we performed whole genome sequencing (WGS) using Oxford Nanopore long read sequencing technology in 349 ocular isolates collected over a one-year period at a tertiary eye care centre in India. Using assembled genomes, we profiled antimicrobial resistance genes (ARGs), studied their association with plasmids and other mobile genetic elements (MGEs) and identified putative resistance mechanisms in the ocular isolates.

Results

Samples from 349 subjects were collected from different parts of the eye including corneal scrapings, corneal buttons, vitreous biopsies, conjunctival swabs, sclero-corneal rims, iris, intraocular lens explant and others. Each sample was subjected to microbiological culture, antimicrobial susceptibility testing (AST) and WGS. Fifty-eight samples that did not meet quality control criteria for high quality genomes (more than 95% completeness and less than 5% contamination) and/or had evidence of mixed infection/contamination were excluded from further analysis. A total of 291 isolates with high quality whole genomes were therefore selected for genotype-phenotype studies. The distribution of pathogens in the cohort, their source and the bioinformatic workflow is given in Figure 1.

Clinical and microbiological profiles of the sequenced bacteria

Out of the 291 isolates, 153 (52.5%) were gram-negative and 138 (47.5%) were gram-positive bacteria. The most frequently sequenced pathogen was *P. aeruginosa* (62; 21.3%) followed by *S. aureus* (60; 20.6%) and *S. epidermidis* (35; 12%) (Fig. 1a). The list of all the bacteria identified in the study; their resistance patterns and their assembly stats are given in Supplementary data 1. Corneal scraping (182; 62.5%) was the primary source of the isolates followed by vitreous biopsy (23; 7.9%), pus (19; 6.5%), half corneal button (11; 3.8%) and others (Fig. 1a, Supplementary data 2). Broadly, resistance to fluoroquinolones was common among both gram positive and gram-negative isolates. In addition, gram-positive isolates were often resistant to macrolides, whereas gram-negative isolates showed frequent resistance to chloramphenicol, minocycline, cefuroxime and trimethoprim-sulfamethoxazole (Supplementary Fig. S1, S2).

Among the 60 *S. aureus* isolates, 29 (48.3 %) were MDR and 9 (15%) were extensively drug-resistant (XDR) (Supplementary data 1). More than 80% of *S. aureus* isolates were resistant to fluoroquinolones and more than 50% to macrolides (Fig. 2a). Over 90% of them were sensitive to linezolid, teicoplanin, nitrofurantoin, vancomycin, tetracycline, daptomycin, rifampin, and tigecycline (Fig. 2a). Similar resistance profiles were also seen in *S. epidermidis* (Fig. 2b). In the 62 *P. aeruginosa* isolates, 28 (45.1%) were MDR and 11 (16.2%) were XDR (Supplementary data 1). A high proportion of *P. aeruginosa* isolates were found to be resistant to trimethoprim-sulfamethoxazole (95.5%), minocycline (80%), and fluoroquinolones (more than 80%) (Fig. 2c). Among fluoroquinolones, the highest sensitivity was observed for ciprofloxacin (62%; 37/60) and levofloxacin (56%; 25/45), while it was the lowest for moxifloxacin (18%; 6/34) (Fig. 2c). On the other hand, most *P. aeruginosa* isolates remained susceptible to amikacin (84.7%), piperacillin tazobactam (78%), and ceftazidime (78.2%). Among 11 *Klebsiella pneumoniae* isolates, 3 (27.2%) were MDR, and 3 (27.2%) were XDR. Among these isolates, resistance against fluoroquinolones (more than 70%), and chloramphenicol (83.3%) was frequently observed (Fig. 2d). Emergence of a susceptible-dose-dependent (SDD) response to tigecycline was noted in two isolates (Fig. 2d). Carbapenem resistance was observed in 9.6% and 36.6% isolates of *P. aeruginosa* and *K. pneumoniae* respectively.

Comparing AST results with genotypes (presence of a corresponding ARG, with or without mutation) identified from assembled genomes revealed varying concordance rates for different antibiotics. In gram-positive isolates, which remained largely sensitive to vancomycin and linezolid, the absence of corresponding ARGs was concordant with the AST results (Supplementary Fig. S3a). 10–12% of isolates resistant to cephalosporins (cefazolin, cefuroxime, and cefoxitin) and macrolides (azithromycin) did not harbor the expected ARGs (Supplementary Fig. S3a). In gram-negative isolates, instances of discordance were seen with respect to cefuroxime, fluoroquinolones (moxifloxacin, gatifloxacin, ofloxacin) and minocycline (Supplementary Fig. S3b). In several isolates, presence of aminoglycoside resistance genes did not confer in vitro resistance. Additionally, mutant ARGs were frequently observed with respect to fluoroquinolone resistance in gram-negative isolates and macrolide resistance in gram-positive isolates.

ARG distribution and their correlation with antimicrobial resistance

Resistance genes identified at 100% sequence identity using Resistance Gene Identifier (RGI) were quantified by FPKM in various bacterial isolates (Fig. 3). 99.3% of these genes had a coverage of more than 95%. Across all gram-positive isolates, aminoglycoside resistance genes

- *aph(3')-IIIa*, *aac(6')-Ie-aph(2'')-Ia*; MDR (quinolones, β-lactams, tetracyclines, peptides) resistance gene - *mgrA*; tetracycline resistance gene, *mepR*; quinolone resistance genes - *arlR*, *arlS*, *norA*; fosfomycin resistance gene - *fosB*; fucidin resistance gene - *fusC*; Trimethoprim resistance genes - *dfrG, dfrC* were abundant (Fig. 3a). In *P. aeruginosa* isolates, the most prevalent were fluoroquinolone and MDR genes *yajC*, *rsmA*, *soxR, mexG* (quinolones and others), aminoglycoside resistance genes *emrE*, *cpxR*, *armR* (macrolide and others); and fosfomycin resistance genes *fosA* (Fig. 3b). *K. pneumoniae* isolates harboured distinct sets of β-lactamase resistance genes compared to other gram-negative species. $bla_{\text{OXA-232}}$, $bla_{\text{SHV-1,}}$ $bla_{\text{CTX-M-15}}$, and $bla_{\text{OXA-1}}$ were prevalent in *K. pneumoniae isolates* whereas *P. aeruginosa* harboured $bla_{\text{OXA-50,}}$ $bla_{\text{OXA-847,}}$ $bla_{\text{OXA-396}}$ and $bla_{\text{OXA-488}}$(Fig. 3b). Other MDR resistance genes that were prevalent in gram-negative isolates included *rsmA, oqxA* (quinolones and others); *kpnF* (macrolide and others) (Fig. 3b).

In the common isolates, *S. aureus and P. aeruginosa* using Spearman's rank correlation analysis, associations between specific ARGs and their corresponding antibiotic resistance phenotypes were analysed for statistical significance. In *S. aureus* (Supplementary data 3), strongest correlations were observed for *tet(K)* with tetracycline resistance (r = 0.99, q < 0.001) and, *mecA* with oxacillin resistance (r = 0.7, q < 0.001). Significant correlations were also observed for *dfrG* with trimethoprim-sulfamethoxazole resistance (r = 0.62, q = 0.001), *msrA* and *mphC* with erythromycin resistance (r = 0.56, q <0.02), and *ermC* with clindamycin resistance (r = 0.5, q = 0.05). In *P. aeruginosa*, strong correlation of cefepime resistance with *rmtF,* $bla_{PAC1,}$ and bla_{PDC-98} (Spearman's r = 0.7, q = 0.001) and moderate correlation of cefoperazone resistance with bla_{OXA-10} (r = 0.663) and bla_{PDC-98} (r = 0.6, q = 0.01), and gentamicin resistance with *rmtf (r=0.6, q=0.02)* (Supplementary data 3) was observed.

Sequence types and AMR signatures in MDR and XDR isolates of *S. aureus, S. epidermidis, P. aeruginosa and K. pneumoniae*

Firstly, to exclude clones/ duplicates, ANI between each of the isolates (*S. aureus, P. aeruginosa*) was compared (Supplementary data 4a and 4b). None of the isolates were a 100% match with another, suggesting the lack of clones/duplicates in the data. Further, exploration of sequence types and their association with infection type/ tropism to specific anatomical sites did not reveal any significant findings (Supplementary data 5a, 5b). This is probably due to the small sample sizes. The distribution of sequence types and their associated AMR signatures is given below.

S. aureus

The 38 MDR and XDR *S. aureus* isolates could be categorized into nine different sequence types (ST) with ST1 (23.6%) and ST22 (21%) being the most frequently identified. Seven of the isolates could not be typed due to uncatalogued alleles in *aroE*, *glpF* and *yqiL.* Among 10 methicillin-resistant *Staphylococcus aureus* (MRSA) isolates in our cohort, seven were *mecA*-positive and belonged to ST1 (n=2), ST22 (n=2; Fig. 4, Supplementary data 6). The remaining three *mecA*-negative MRSA isolates did not carry *mecC, mecB*, or other β-lactamase genes but were resistant to oxacillin. These *mecA* negative MRSA strains belonged to sequence types ST1, ST672 and an unassigned ST. Notably, this unassigned ST, which has now been assigned to ST9578 and clonal complex CC30 by pubMLST with an allele in *yqiL(A->G),* was resistant to vancomycin and teicoplanin as well. In four macrolide resistant isolates, no corresponding macrolide resistance gene was identified. Additionally, macrolide resistance signatures were found to be ST-specific, with ST22 *S. aureus* harboring only the *ermC* gene, while resistance in ST672 was associated with the presence of *mphC/msrA* (Fig. 4). All *S. aureus* isolates harbored several fluoroquinolone resistance-associated genes, including *norA, arlS, arlR, mgrA, gyrA, norC, sdrM,* and *parC*. Importantly, the presence of ARGs for Daptomycin (*vanT*) did not confer phenotypic drug resistance (Fig. 4).

S. epidermidis

The 21 MDR and XDR *S. epidermidis* isolates were classified into 11 STs, with ST35 (4/21, 19%), ST17 (3/21, 14.2%), and a previously unreported ST1258 (4/21, 19%), carrying an uncatalogued *pyrR* allele, being the most prevalent (Supplementary data 1). Among the ST1258 isolates, one was XDR, while the other three were MDR. Of the seven isolates resistant to both benzylpenicillin and oxacillin, six harbored *mecA*, and two co-harbored *mecI* and *mecR1* (Fig. 4). Isolates resistant to either azithromycin or erythromycin harboured *mphc/msra* or *ermC* indicating these as genomic determinants for macrolide resistance in *S. epidermidis* (Fig. 4).

P. aeruginosa

Among the *P. aeruginosa* isolates, 36 were either MDR or XDR and belonged to 20 different STs with ST3755 (9) being the most frequently identified (Supplementary data 1). High-risk *P. aeruginosa* isolates belonging to sequence type ST664 exhibited extensive drug resistance (Fig. 5a). These isolates were resistant to piperacillin, cefoperazone, carbapenems (imipenem, meropenem), cefepime, ceftazidime, all classes of fluoroquinolones, aminoglycosides, minocycline, and chloramphenicol. Genomic analysis revealed that all three ST664 isolates harbored the bla_{PAC-1}, bla_{OXA-10}, bla_{PDC-98}, and *rmtF* resistance determinants, which were exclusively present in this sequence type (Fig. 5a). Both *P. aeruginosa* ST308 isolates in our

cohort carried either *bla*$_{NDM-1}$ or *bla*$_{NDM-5}$. ST480 isolate was the only isolate in our cohort that harbored bla$_{DIM-1}$ along with *bla*$_{NDM-1}$, *bla*$_{OXA-395}$, and *bla*$_{PDC-19a}$, and exhibited resistance to cefazolin and cefuroxime (Fig. 5a). In another case, *P. aeruginosa* (ST1527) carrying AmpC-type β-lactamase *bla*$_{PDC-171}$ and *bla*$_{OXA-50}$ exhibited resistance to broad-spectrum cephalosporins such as cefoperazone/sulbactam ceftazidime, as well as piperacillin, ticarcillin, imipenem, and meropenem (Fig. 5a).

K. pneumoniae

Lastly, among the 11 *K. pneumoniae* isolates, ST231 (3/11) was the most common with two of them exhibiting XDR. Though all the isolates of this ST harbored *bla*$_{OXA-232}$, *bla*$_{SHV-1}$, *bla*$_{CTX-M-15}$, and *ompK37*, XDR strains carried multiple bla$_{OXA-232}$ copies, in contrast to a single copy in the sensitive isolate. Another high-risk isolate belonging to ST395-1LV showed resistance to all tested antibiotics including tigecycline. This isolate harboured *bla*$_{NDM-1}$, *bla*$_{NDM-5}$, and *qnrB1,* in addition to other ARGs harboured by XDR isolates (Fig. 5b). In XDR isolates lacking *bla*$_{OXA-232}$, *bla*$_{OXA-1}$ was present, with resistance further increasing when *bla*$_{OXA-1}$ co-occurred with *bla*$_{NDM-5}$. Additionally, genes like *acrB*, ***aac(6')-Ib-cr6***, and mutant *ramR* were found in MDR strains contributing to the resistance against quinolones, β-lactams, glycylcycline, rifamycin, and phenicols (Fig. 5b). One isolate which showed resistance to all quinolones harbored *AAC(6')-Ib-cr6* and *A19V* mutation in *ramR*.

Plasmid-encoded ARGs network reveals ESBL gene clusters in Enterobacteriales

In order to understand plasmid content in the isolates, geNomad was used for plasmid identification in the bacterial genomes followed by annotation using PlasmidFinder. 29 out of 60 *S. aureus* isolates harboured plasmids. Whereas 20 out of 35 and 10 out of 62 isolates of *S. epidermidis* and *P. aeruginosa,* respectively, were found to have plasmid content. Additionally, plasmid associated ARGs were found in eight *K. pneumoniae* and two *Acinetobacter baumannii* (*A. baumannii*) isolates. *K. pneumoniae* had the highest plasmid count/isolate (22 from 8 isolates), followed by *P. aeruginosa* (18 from 10 isolates). 15 *K. pneumoniae* and 10 *P. aeruginosa* plasmids carried conjugative genes annotated by RGI, indicating a high transfer potential. Supplementary data 7 provides a description of the most frequently observed plasmid-associated ARGs in each ocular isolate, along with their corresponding ARG classes and the antibiotic categories to which they confer resistance to. Further, a plasmid-ARG network was generated from 146 plasmids. Network topology showed that plasmids were clustered by ARGs according to antibiotic classes (Fig. 6a). *P. aeruginosa* plasmids carrying macrolide and fluoroquinolone resistance genes formed a motif hub (clusterA) connecting *rmtb*, *bla*$_{TEM-1}$, hub genes linking to conjugative *K.*

pneumoniae plasmid (clusterB) (Fig. 6a). Cluster B comprising multiple beta-lactamase genes (*bla*$_{SHV-1}$, *bla*$_{oxa-9}$), with hub as *bla*$_{CTX-M-15}$ was in turn associated with cluster C having *bla*$_{OXA-1}$, *qacEdelta1*, *sul1* and other macrolide, tetracycline and aminoglycoside resistance genes. These genes were shared by multiple conjugative plasmids of *Escherichia coli* (*E. coli)* and *K. pneumoniae*, suggesting potential co-transfer. There were clusters comprising shared genes between conjugative plasmids of *A. baumannii–K. pneumoniae* and *Enterobacter cloacae* (*E. cloacae)–K. pneumoniae–P. aeruginosa*. *A. baumannii* harbored *bla*$_{CTX-M-163}$, *bla*$_{TEM-247}$, and *catI*, which were linked to *rmtF* and ***aac(6')-Ib*** of *K. pneumoniae* (Fig. 6a). The *ermC* gene was associated with a cluster of *S. aureus* isolates with macrolide resistance. In contrast to the gram-negative isolates, most plasmids in the gram-positive isolates were not conjugative except for fluoroquinolone carrying plasmids in *S. epidermidis* (Supplementary Fig. S4).

High sequence identity between plasmids carrying *bla*$_{OXA-1}$ and *bla*$_{CTX-M-15}$ in *E. coli* and *K. pneumoniae*

To further investigate the potential co-transfer of *bla*$_{OXA-1}$ and *bla*$_{CTX-M-15}$ suggested by network analysis, we analysed the genetic environments and sequence similarity of plasmids of MDR isolates of *E. coli (*pRSB107*)* and *K. pneumoniae* (pKP91)*.* A high degree of sequence identity (99.9%, with both plasmids being covered at 100%) was noted, especially in the IncFII plasmid (Fig. 6b). IncFII plasmids were present in ST101 in *K. pneumoniae* and ST131 in *E. coli*. These two lncFII plasmids carried *bla*$_{OXA-1}$, which co-localized with *bla*$_{CTX-M-15}$ and ***aac(6')-Ib-cr*** genes in both the species. These were flanked by the same MGEs including IS6 elements, transposon Tn6292, and multiple TnpA genes (Fig. 6c). This high sequence identity and shared plasmid type between these two species suggests a possible plasmid mediated MDR gene transmission event between *E. coli* and *K. pneumoniae*.

Plasmid content in high-risk *K. pneumoniae* (ST395-1LV) isolate

On interrogation of the genetic architecture of the three plasmids harboured by high-risk *K. pneumoniae* isolate belonging to ST395-1LV, one belonged to the IncFII(k) type where NDM-1 was co-localized with *BRP* (MBL) and was flanked by IS6 and Tn6292 along with multiple *tnpA* and *tnpR* elements (Fig. 7a). The same plasmid harboured *bla*$_{CTX-M-15}$ in the adjacent resistance region along with ISNCY, *tnpA*, *insA3* and others. The second plasmid harboured *bla*$_{NDM-5}$, *brp(mbl), ermB, qacEdelta1, rmtb, bla*$_{TEM-1}$*, mrx/mphA* with IS6 and Tn6292 transposons in their flanks (Fig. 7b). In the third plasmid (type ColKp3), *bla*$_{OXA-232}$ was flanked by Tn6284 and Tn2012 transposons (Fig. 7c). Unlike the other two plasmids which carried multiple ARGs, this plasmid contained only *bla*$_{OXA-232}$.

Other Mobile Genetic Elements

To further characterize other MGEs contributing to antimicrobial resistance dissemination, we analyzed the distribution of integrons, transposons, and replicons across the four predominant ocular bacterial pathogens in our cohort.

Among the 60 *S. aureus* isolates, resistance-associated transposons were detected in 41 isolates (68.3%). Tn552 was the most clinically relevant transposon, found majorly on plasmids in MDR and XDR isolates (ST672, ST1, and others). Tn552-harboring plasmids carried multiple resistance genes including aminoglycoside resistance determinants (*ant(6)-Ia, aph(3')-IIIa*), β-lactam resistance genes (*blaR1, blaZ*), macrolide resistance genes (*mph(C), msr(A))*, *cadD*, tetracycline resistance (*tet(38)*), and efflux pump genes (*lmrS, mepA*). Tn4001-harboring plasmids predominantly carried aminoglycoside resistance genes (*aac(6')-Ie, ant(4')-Ia*) along with *blaR1, blaZ*, *tet(38), tet(K)*, and efflux-mediated resistance determinants. No integrons were identified in *S. aureus* isolates. Of the 34 *S. epidermidis* isolates, 24 (70.6%) harbored transposable elements, all of which were associated with ARGs. The most prevalent transposons were Tn6191 (n=22, 46.8%), Tn4001 (n=9, 19.1%), and Tn6292 (n=6, 12.8%). Eight isolates harbored transposons on plasmids. Tn6191-harboring plasmids carried *mecA*, *blaR1, blaZ*, trimethoprim resistance (*dfrC, dfrG*), fosfomycin resistance (*fosB*), *cadD*, tet(K), *fusC* and others. Integron elements were rare in *S. epidermidis*, with only two integrons (In2-10 and In498) detected in a single XDR isolate belonging to ST1255 along with Tn21 transposon, bla_{TEM-1} and other resistance genes.

In *P. aeruginosa* isolates, 12 (19.4%) harbored integron elements, with a total of 24 integrons detected. The most prevalent integron class was In498 (n=9, 37.5%), followed by In933 (n=4, 16.7%) and In221 (n=3, 12.5%). BacAnt analysis identified 20 distinct transposable elements across 16 isolates (25.8%), with 12 isolates carrying ARGs associated with transposons. Only one isolate (ST357) harbored plasmid-borne transposon Tn6291 accompanied by integron In510, carrying *aadA2,* bla_{NDM-5}, ble_{MBL}, *dfrA12*, and sulfonamide resistance genes. *K. pneumoniae* exhibited the highest burden of resistance-associated MGEs, with 10 of 11 isolates (90.9%) harboring resistance-linked transposons. Of these, 7 (70%) were plasmid-borne, highlighting the horizontal gene transfer potential. Tn6292 was the most frequently observed transposon, typically accompanied by integron In498 on plasmids. These MGEs carried diverse resistance determinants including β-lactam resistance: $bla_{CTX-M-15}$, bla_{OXA-1}, bla_{TEM-1}, bla_{NDM-1}, bla_{NDM-5}, ble_{MBL}, aminoglycoside resistance: *aac(6')-Ib-cr* (quinolone/aminoglycoside bifunctional), *aadA2*, *aph(3')-Ia, aph(3'')-Ib, aph(6)-Id, arr-2* , *rmtF1*, *qnrB1, dfrA12, dfrA14*, *sul1, sul2*, *mph(A), catB, and tet(A)*.

The XDR isolate ST395-1LV harbored transposons Tn2012 and Tn21 accompanied by integrons In49 and In498 respectively. Similarly, the XDR isolate ST231-1LV harbored transposons Tn6229 and Tn21 with integrons In498 and In240, carrying *rmtF1*, chloramphenicol resistance *catA1, catB*, *aadA2, arr-2*, *mph(A), and erm(B*). The same isolate harbored the Tn2003 transposon along with multiple β-lactam resistance genes, including *bla*$_{CTX\text{-}M\text{-}15,}$ *bla*$_{SHV}$, and others. Plasmids belonging to ST231-1LV carried key conjugative transfer genes, including *MOBF* and *traI*. Similarly, ST395-like plasmids encoded an extensive repertoire of conjugation-associated genes (*traL, traE, traK, traV, virB4, traW, traU, trbC, traN, traF, traH, traG,* and *MOBF*), located on Tn2012 carrying plasmid contig. The co-localization of carbapenemase genes, ESBLs, and aminoglycoside-modifying enzymes on conjugative plasmids highlights potential for horizontal transfer. A comprehensive list of these MGEs is provided in Supplementary data 8.

Vancomycin Resistant *S. aureus* (VRSA)- ST9578 and its resistance mechanism

Phylogeographic analysis revealed that the *mecA*-negative VRSA (ST9578) did not cluster with any of the isolates from our cohort but rather shared a common ancestor with ST30, previously isolated from human vaginal sample in the UK in 2015 (BioSample: SAMEA3529260) (Fig. 8a, Supplementary Fig. S4). ST30 and ST9578 differed in three housekeeping genes: *pta, tpi,* and *yqiL*. Both genomes harbored *norC*, *tet(38)*, *mepA/R*, *mgrA*, *arlS/R*, *vanT*, *lmrs*, *blaZ*, mutated *murA* (D278E, E291D), and mutated g*lpT* (A100V, V213I). However, this isolate from our cohort carried additional mutations in *gyrA* (S84L) and *parC* (S80F). Of the 60 *S. aureus* isolates, this was the only strain resistant to Linezolid. The 23S *rRNA*, *rplC*, *rplD*, and *rplV* genes have been shown to accumulate mutations that cause Linezolid resistance[24]. Therefore, these gene sequences were studied for variations using multiple-sequence alignment. No mutations were identified in the 3 protein coding genes but interestingly a mutation of G1549A was found in all the 6 copies of 23S rRNA coding gene (Fig. 8b), suggesting the selection of this mutation for Linezolid resistance.

Comparative genomic analysis identifies putative AMR associated genes and mutations in *P. aeruginosa, and S. aureus*

Fluoroquinolone resistance in *P. aeruginosa*

A total of 33,495 genes were identified in the genomes of *P. aeruginosa* (showing >99% ANI, n = 33) isolates present in our cohort. These isolates exhibited a gradation in resistance to fluoroquinolones i.e, 88% (29/33) of the strains were resistant to moxifloxacin, 52% (17/33) to gatifloxacin, 50% (15/30) to ofloxacin, 42% (8/11) to levofloxacin and 39% (13/33) to ciprofloxacin. In 6 isolates that were resistant to all the fluoroquinolones, a gene encoding for a protein of

unknown function was identified and this was not present in any of the sensitive isolates (n = 38). Structure-based analysis using hhPred showed that this protein had a *parB*-like domain in the N-terminal half of the protein (Supplementary Fig. 5B). This is similar to the long-range gene expression regulator protein KorB that is found in broad-host range multidrug resistant plasmid RK2[25,26]. Several canonical OB (operator for KorB) sites were seen in the flanking 100-Kb sequence of this gene, supporting its role in AMR (Supplementary data 9)[27]. Additionally, potential resistance mechanisms to aminoglycosides are represented in the Supplementary figure 5B.

Cephalosporin sensitivity in *mecA* positive *S. aureus* isolates

Comparing the *S. aureus* isolates resistant and sensitive to the cephalosporins - cefuroxime and cefazolin, we found that both the resistant and the sensitive isolates carried the *mecA* gene. On screening for any possible inactivating mutations, we identified a S225R mutation in 4 isolates that were *mecA* positive but sensitive to cefuroxime ($p < 0.05$, chi-squared test) and cefazolin ($p = 0.0581$, chi-squared test). Further, homoplasy analysis (CI = 0.17) corroborated the significance of the variant detected. Interestingly, a phage locus was also identified in 5 out of 11 sensitive isolates but not in the resistant ones. Mutations in *mecI*/*mecR1*/*blaR1* regulatory systems have also been observed in relation to resistance or sensitivity (Supplementary Fig. 5C). Resistant *mecA* positive isolates belonged predominantly to CC8, whereas sensitive *mecA* positive isolates were mainly CC15, suggesting the possibility of additional lineage-specific regulatory mechanisms.

Discussion

Ocular infections, in many respects, can reflect the AMR burden of a region or a country. Given that these infections are often acquired from environmental sources or commensal flora of skin and mucus membranes, they can reflect the prevailing resistome of the local community and environment. It is therefore important to track pathogen evolution, especially in the context of emerging XDR strains associated with ocular infections. Whole-genome sequencing offers unparalleled insights here, enabling detailed investigation into the mechanisms behind infection outbreaks, pathogen evolution, and ARG dissemination[23]. In this large-scale study focused on AMR in ocular infections from India, we sequenced bacterial isolates using Oxford Nanopore Technology (ONT), generating high-quality genome assemblies from 291 samples.

Analysis of these genomes revealed several notable findings. Among *S. aureus* isolates, ST22 and ST1 were the predominant sequence types. This contrasts with findings by Johnson et al. (2021), where analysis of 163 ocular *S. aureus* isolates from Rochester, New York, identified

sequence types ST5 (21%), ST8 (15%), and ST30 as the dominant lineages[28]. Similarly, in an 8-year surveillance study by Andre et al. (2023), clonal complexes CC5 and CC8 were common among ocular isolates in Massachusetts[29]. A recent genomic analysis published in 2025, looked at 1,710 *S. aureus* genomes from 58 countries, also identified ST5 and ST8 as the predominant sequence types reported from the USA, Australia, and Kenya[30]. ST22 (EMRSA-15), originally isolated from the UK, has become a hospital-associated MRSA lineage with many recent reports coming from Asia[31,32], and has a strong potential to replace other previously epidemic MRSA clones. Our phylogeographic analysis with 185 publicly available *S. aureus* genomes revealed that ST22 is geographically restricted to Asia, whereas ST1 exhibited a different pattern with global distribution, a characteristic of community-associated *S. aureus* lineage.

In contrast, ST3755, the most common *P. aeruginosa* sequence type identified in our cohort, appears to be more prevalent in Asia compared to the West, with two studies from China reporting it in XDR and hypervirulent *P. aeruginosa* isolates[33,34]. High-risk clones like ST664, associated with MDR and nosocomial transmission[35] and ST1527, exhibiting resistance to all tested antibiotics are other notable findings. These findings highlight the region-specific differences in the distribution of various bacterial strains with potential implications on regional antibiotic policies.

In our analysis of three *K. pneumoniae* ST231 isolates, the susceptible strain carried a single copy of $bla_{OXA-232}$, whereas the two resistant strains harbored multiple copies. This aligns with previous reports, which suggest that $bla_{OXA-232}$ exhibits a weaker carbapenemase activity and the resistance is therefore proportional to the copy number of $bla_{OXA-232}$ [36,37]. We observed shared genetic architecture of ESBL genes bla_{OXA-1} and $bla_{CTX-M-15}$ in plasmid regions *E. coli* and *K pneumoniae* isolates. A recent study had also reported the co-localization of similar resistance genes and shared genetic environment contributing to MDR in *E. coli* and *K. pneumoniae* isolated from hospital wastewater samples[38]. While our genomic evidence demonstrates genetic similarity consistent with mobile element transfer, experimental verification through conjugation assays would be required to definitively confirm the transfer event. The association of transposons Tn6292 and Tn5393c with bla_{NDM} and $bla_{CTX-M-15}$ in *K. pneumoniae and P. aeruginosa* aligns with global surveillance data showing these transposons as primary vehicles for carbapenemase spread in Enterobacterales[39,40]. *K. pneumoniae* exhibited the most complex mobilome with predominantly plasmid-associated transposons and conjugative elements. The prevalence of plasmid-borne Tn2012 and Tn21, particularly within high-risk lineages like ST231 and ST395, highlights a dangerous trend toward the consolidation of carbapenemase and aminoglycoside resistance genes. Crucially, the co-localization of these resistance determinants with complete

conjugative machinery (*tra* and *MOB* systems) suggests a potential for rapid horizontal dissemination across hospital environments.

Comparison of the AST results with the sequencing information led to the finding of several instances of discordance between the genotype and the phenotype. The absence of a corresponding gene to a resistance phenotype indicates possibilities such as modifications of target sites, overexpression of auxiliary mechanisms, gain of function mutations in existing genes or the presence of hitherto undiscovered resistance genes/ mechanisms. Similarly, the absence of resistance in the presence of a known ARG possibly indicates inactivating mutations in the gene or previously unidentified mechanisms enabling sensitivity. Our investigations in this line resulted in discovery of several putative resistance/sensitivity mechanisms. The *S. aureus* ST9578 isolate was also the only isolate resistant to linezolid in our cohort. Linezolid acts by binding to the 50S ribosome and preventing the formation of the initiation complex and earlier studies have shown resistance to linezolid through accumulation of mutations in domain V of 23S rRNA[41]. In our isolate, we identified a previously unreported mutation (G1549A) in domain III (important for inter-domain interactions) of 23S rRNA in all six copies of the gene encoding 23S rRNA and this warrants further investigation. The resistance phenotype in this isolate correlated with the patient's history of chronic hospitalisation for renal disease and recurrent antibiotic exposure, resulting in emergence of this hospital-acquired VRSA sequence type. A S225R coding mutation was identified in the *mecA* gene in the *S. aureus* isolates sensitive to cefuroxime and cefazolin, suggesting its role in rendering the protein inactive for cephalosporin resistance. Further, we also found a phage loci only in the sensitive isolates. It is possible that the stress caused by the antibiotic induces these phages thereby killing the cells. Instances, such as these, where identification of an ARG does not translate into *in vitro* or *in vivo* resistance, highlight the limitation of using gene-based testing for clinical decision making.

High fluoroquinolone resistance was observed among ocular pathogens in our cohort. This can be attributed to a combination of local antibiotic usage practices and microbial resistance mechanisms. In India, gatifloxacin and moxifloxacin are frequently available over the counter and are often used as prophylaxis after cataract surgery, while ciprofloxacin is routinely prescribed empirically for ocular infections. In addition, unregulated availability also enabled systemic fluoroquinolone abuse. This widespread exposure exerts strong selective pressure favoring evolution of resistant strains. The presence of mutant ARGs in fluroquinolone resistance genes is consistent with the presence of this selection pressure. Further, a pangenome comparison done to investigate fluoroquinolone resistance in *P. aeruginosa* revealed several genes of unknown

function exclusive to resistant isolates. On further investigation, we identified a gene encoding a KorB-like protein containing a ParB-like domain in the N-terminal followed by a long loop and an uncharacterised C-terminal domain in isolates that were resistant to all the fluoroquinolones. Unlike *KorB*, which is present in the RK2 plasmids, this gene is present in the chromosome. On examining the flanking genes, it is evident that this gene is present in a transposon cluster containing multiple AMR genes. We found OB sites upstream of genes involved in Horizontal Gene Transfer (HGT) such as integrases, site-specific recombinases and transposases. Further, we identified OB sites upstream of various AMR genes, universal stress response protein - UspE encoding gene and genes encoding proteins of unknown function. As this KorB-like protein is a transcriptional regulator, further studies involving transcriptome profiling may aid in elucidating this resistance mechanism better.

Our study, though largest from India to date, is not exhaustive. The number of isolates sequenced, for several species, was in single digits, precluding their detailed analysis. *Streptococcus pneumoniae,* a common ocular pathogen, is under-represented in this cohort. Exclusion of mixed infections from the study ignores a critical aspect of *in vivo* antibiotic sensitivity. Though putative resistance/sensitivity mechanisms were identified, confident interpretations could not be made due to lack of mechanistic evaluation through functional studies. In addition, limitations inherent to the current resistance gene databases should also be kept in mind while interpreting the results of the study.

In conclusion, our study demonstrates a high burden of in vitro resistance to fluoroquinolones among ocular pathogens, highlighting the need to revisit the empirical use of this antibiotic class in ocular infections. The identification of emerging XDR isolates is particularly concerning. Although whole-genome sequencing does not provide clinically actionable information within the routine clinical timelines, it offers critical insights into the genetic basis of resistance and supports the development of evidence-based treatment strategies and antimicrobial stewardship policies. With decreasing costs of NGS, integration of genomic surveillance into clinical practice is becoming increasingly feasible. Finally, our findings add additional evidence to the fact that pathogens exhibit region-specific variations in sequence types and AMR genes, further emphasizing the critical need for genomics-based surveillance efforts, especially in LMICs.

Methods

Bacterial isolates

This was a prospective study that was approved by the Institutional Review Board (LEC 11-16-112 & IEC-101/2023) and the research adhered to the tenets of the Declaration of Helsinki. Ocular tissue samples including corneal scrapings, vitreous biopsies, conjunctival swabs or pus from the abscess, were collected from patients after informed consent, seen between May 2023 - April 2024 and who had a clinical diagnosis of ocular infection (microbial keratitis / conjunctivitis / endophthalmitis, orbital cellulitis or abscess) following clinical examination by an ophthalmologist during their visit to the institute. All samples were collected under aseptic conditions using sterile instruments in the operating theatre or outpatient clinic. The specimens were immediately transported to the microbiology laboratory and processed according to the institutional microbiological protocol for ocular infections. Briefly, the samples were smeared onto two slides for direct microscopic examination by 10% potassium hydroxide + 0.1% Calcofluor white (KOH+CFW) and Gram stain. They were also inoculated directly onto 5% sheep blood agar, 5% sheep blood chocolate agar, Sabouraud dextrose agar, potato dextrose agar and brain-heart infusion broth as required. All media were incubated at 37°C for 7 days. In case of positive cultures, the bacteria were further subjected to identification by conventional biochemical tests and/or Vitek 2 Compact (bioMérieux, France) automated identification systems as well as antibiotic susceptibility testing. Only clinically significant isolates that correlated with smear findings and clinical presentation were included in the final microbiological analysis.

Antimicrobial susceptibility testing (AST)

Antimicrobial susceptibility of the isolates was determined by minimum inhibitory concentration (MIC) using E-test (bioMérieux, France) / Vitek-2 AST cards, according to the manufacturer's instructions. Bacterial inocula were prepared from fresh overnight cultures and adjusted to a turbidity equivalent to a 0.5 McFarland standard. For the E-test, standardized inocula were swabbed uniformly onto Mueller–Hinton agar plates, and antibiotic gradient strips were applied. Plates were incubated aerobically at 35–37 °C for 16–18 hours, after which MIC values were read at the point where the ellipse of inhibition intersected the scale on the strip. For isolates tested using the VITEK-2 system, bacterial suspensions were loaded into the appropriate AST cards and processed automatically by the instrument, which generated MIC values based on growth kinetics. Clinical and Laboratory Standards Institute guidelines (2020) were followed in performing the tests and interpretation. Quality control procedures were performed using recommended reference strains to ensure accuracy and reliability of susceptibility testing. The following antibiotics were tested for gram-positive bacteria: oxacillin, cefoxitin, vancomycin, teicoplanin, linezolid, clindamycin, erythromycin, azithromycin, tetracycline, gentamicin, ciprofloxacin,

levofloxacin, moxifloxacin, gatifloxacin, trimethoprim-sulfamethoxazole, and chloramphenicol. Detection of methicillin resistance among staphylococci was inferred using oxacillin and cefoxitin susceptibility results as per CLSI recommendations. For gram-negative bacteria, the following antibiotics were tested: ampicillin, piperacillin, piperacillin-tazobactam, ceftazidime, cefepime, cefotaxime, ceftriaxone, aztreonam, imipenem, meropenem, doripenem, amikacin, gentamicin, tobramycin, ciprofloxacin, levofloxacin, colistin, and tigecycline. Moxifloxacin MICs were determined using the E test for comparative purposes only, alongside other fluoroquinolones. In the absence of Clinical & Laboratory Standards Institute (CLSI)-endorsed breakpoints for *P. aeruginosa*, the MICs were interpreted using surrogate (Enterobacterales) criteria to allow intra-study comparison of relative fluoroquinolone activity. All susceptibility results were categorized as susceptible, intermediate, or resistant according to CLSI interpretive criteria. Where applicable, results were further analyzed to determine patterns of multidrug resistance among the isolates. As frank resistance to vancomycin and teicoplanin is rare, the ST9578 isolate underwent repeat testing on separate occasions using freshly subcultured colonies using both E test (bioMérieux, France) and Kirby–Bauer disk diffusion. Additional details regarding sample processing and AST can be found at https://data.ccmb.res.in/apsi/protocol/.

Nanopore library preparation

Genomic DNA was isolated from these cultured isolates using the QIAamp DNA minikit (Qiagen, Germany) and later quantified with Qubit 1X dsDNA HS Assay Kit by using Qubit 4 Fluorometer (Invitrogen by Thermo Fisher Scientific). DNA samples with concentration ≥35 ng/µl were considered for whole genome library preparation using Native Barcoding Kit 96 V14 (SQK-NBD114.96) (Oxford Nanopore Technologies, ONT) as per the manufacturer recommendations. Briefly, 400ng of DNA from samples passing QC was used for DNA repair and end-prep, native barcode ligation, adapter ligation and clean-up steps. The prepared library was quantified using the Qubit 1X dsDNA HS Assay Kit, and library size was analyzed on TapeStation 4200 (Agilent) using gDNA screenTape. 50 fmol of the pooled library were loaded onto a PromethION flow cell (R10.4.1) (ONT) and sequenced on a PromethION 24 (ONT). Low-yield isolates were subjected to top-up sequencing to achieve a target of approximately 200× coverage based on bacterial genome sizes.

Data processing

Raw nanopore sequencing data generated on R10.4.1 flow cells using PromethION (ONT) was collected at sampling rates of 4 kHz or 5 kHz. The raw signal data (FAST5/POD5 files) were basecalled using Dorado (v0.7.1, ONT PLC, 2024) with the super-accuracy (SUP) models

optimized for the respective sampling rates: *dna_r10.4.1_e8.2_400bps_sup@v4.1.0* for 4 kHz and *dna_r10.4.1_e8.2_400bps_sup@v5.0.0* for 5 kHz data. Base called reads were subjected to quality control using NanoPlot (v1.41.6)[42] to assess read length distribution, quality scores, and yield statistics.

Taxonomic classification was done using Kraken2[43] with 'k2_pluspfp_20230314' as the reference database. Subsequently, the dorado base called reads were also assembled into contigs using Canu (v2.2)[44] with default parameters (raw error rate = 0.30, corrected error rate = 0.045, minReladlength 1000bp and minimum overlap length = 500 bp). The estimated genome size for each isolate was specified in the canu command to enable better calculation of assembly statistics. Inspector[45] and CheckM[46] were used to check the assembly quality. High quality genomes with more than 95% completeness and less than 5% contamination were considered for further analyses. Average Nucleotide Identity (ANI) was computed using FastANI[47]. The resulting contigs were used for downstream genomic characterization and antimicrobial resistance gene analysis. Multilocus sequence typing (MLST) was determined using MLST (https://github.com/tseemann/mlst) and pubMLST[48]. Kleborate (https://github.com/katholt/Kleborate/) was used to type *K. pneumoniae* isolates.

Annotation of ARGs and MGEs

To identify ARGs in assembled genomes, the Resistance Gene Identifier (RGI) tool (https://github.com/arpcard/rgi) was used against the Comprehensive Antibiotic Resistance Database (CARD) database[49]. Minimap2[50] was used to align reads to contigs. ARG abundance was quantified based on Fragments Per Kilobase of transcript per Million mapped reads (FPKM) using Samtools[51] and bedtools[52].

$$FPKM = \frac{ReadsMapped}{GeneLength \times \frac{TotalReads}{1{,}000{,}000}}$$

ReadsMapped corresponds to the number of reads mapping to ARG, gene length corresponds to length of ARG, and TotalReads corresponds to the total number of bacterial reads per sample. Minimap2[50] was used to align reads to contigs. In-house python scripts were written to compare the phenotypic outcomes from antibiograms with ARGs identified from the genomes. ARGs with 100% sequence identity were used as the primary cutoff. When phenotypic resistance was observed without 100% identity, ARGs with lower sequence identity were identified and designated as mutated ARGs. geNomad (v1.8)[53] and Plasmidfinder[54] were used to annotate contigs as plasmids from the assembled genomes. The normalised abundances of plasmid-associated ARGs were processed and transformed into Spearman correlation matrix using Hmisc

package in R. Associations with p-value less than 0.05 were selected for further analysis. Based on filtered associations, a plasmid-ARG adjacency matrix was generated and handled using phyloseq[55] and igraph. The undirected graph pertaining to the network connectivity was obtained and visualized in Gephi v0.10.1 using ForceAtlas2 layout[56]. To further annotate MGEs in plasmids, ISfinder (https://isfinder.biotoul.fr/) was used to annotate insertion elements in the identified plasmid. BacAnt v3.4.0 (https://github.com/xthua/bacant) was used to annotate integrons, transposons and replicons. Proksee[57] was used to visualize MGEs and ARGs in plasmids. Microbiome[58], ggplot and ggpubr packages in R were used for downstream analysis and data visualization.

Phylogeographic analysis

60 in-house *S. aureus* isolates were analysed alongside 185 publicly available reference genomes retrieved using the NCBI-datasets command-line tools. Genome assemblies were annotated using Prokka (v1.12) with default parameters[59]. ARGs and sequence types were identified for 185 reference genomes using the pipeline mentioned in the previous section. Pangenome analysis was conducted using Roary (v3.11.2)[60], generating core genome alignments from annotated assemblies. A maximum-likelihood phylogenetic tree based on the core genome alignment was constructed using RAxML (v1.1) with the GTR+G substitution model[61]. The resulting tree was visualized and annotated using iTOL[62]. Additionally, SCCmecFinder[63] was employed to determine the SCCmec types among the *S. aureus* isolates.

Mutation analysis of genes known for antibiotic resistance *a priori*

The gene sequences were extracted from the assembled genomes of both resistant and the sensitive strains using a custom python script. Multiple sequence alignment was done using MAFFT in MEGA X software[64]. Mutations present in the resistant genomes, either causing a nucleotide-change or an amino-acid-change were identified, by careful inspection of the entire aligned sequence.

Genome-wide comparison of resistant and sensitive isolates

To identify putative genes or mutations associated with antibiotic resistance in strains where no known ARGs were found, genome-wide comparison between the resistant strains and the sensitive strains to a particular antibiotic was done. Firstly, closely related genomes were identified using an ANI cut-off of more than 99%. The pan-genome analysis pipeline using amromics[47] was used to identify the genes that are present in the closely related genomes. A two-by-two matrix was constructed for every gene with the following criteria, a - number of sensitive

genomes absent from, b - number of resistant genomes absent from, c - number of sensitive genomes present in, and d - number of resistant genomes present in. From this matrix, odds ratio was calculated and Fisher's exact test was used to calculate the p-values for the association of a gene with antibiotic resistance. To identify the amino acid changes associated with antibiotic resistance, the alignment was done between all the similar protein sequences using amromics[65]. The amino acid changes were extracted using a custom python script and a two-by-two matrix was constructed as above for the absence or presence of mutations in sensitive or resistant genomes respectively. From this matrix, odds ratio was calculated and Fisher's exact test was used to calculate the p-values for the association of a mutation with antibiotic resistance.

Gene-Neighbourhood analysis

The gene-neighbourhood was assessed for every putative gene associated with antibiotic resistance by taking 10 genes upstream and downstream to a gene of interest using custom python scripts and with the Prokka annotated .gff files as the input. The genes were classified according to their position of occurrence within a cluster. The genes that showed similar order of occurrence in all resistant genomes were taken as genes involved in auxiliary processes such as horizontal gene transfer and were eliminated.

Homoplasy analysis

For the amino acid changes that were identified to be associated with antibiotic resistance, homoplasy analysis was done to assess their potential convergent evolution across phylogenetically distinct strains. Firstly, the phylogenetic tree for all the strains of a species was drawn using a list of 45 highly conserved genes. The consistency-index (CI) values were calculated for each amino-acid change, using a similar calculation to phangorn[66] using a custom python script. The mutations showing less than 0.3 CI were taken as homoplasic mutations.

Statistics and Reproducibility

Spearman's rank correlation analysis was used to assess associations between ARGs and antibiotic resistance phenotypes in *S. aureus* and *P. aeruginosa*. Correlation coefficients (r) and p-values were computed using the cor.test function (method = "spearman") in R (version 4.5.1). P-values were adjusted for multiple comparisons using the Benjamini–Hochberg FDR method (p.adjust); adjusted p-values are reported as q-values. Correlations with $q < 0.05$ and $|r| > 0.5$ were considered statistically significant. For the identification of putative ARGs odds ratio was calculated and Fisher's exact test was used to calculate the p-values for the association of a mutation with antibiotic resistance. Analysis scripts are available at

https://github.com/apuratha/ocular-amr and https://github.com/Shyamili09/ARGs-Antibiogram-comparison.

Data Availability

All genomes assembled as part of this work are openly available to researchers across the world and can be accessed at NCBI (PRJNA1267791) and https://doi.org/10.5281/zenodo.18996254[67]. The source data used for generating the figures is available in the folder 'Supplementary data 10' provided along with this paper.

Code Availability

The custom python scripts are available at https://github.com/apuratha/ocular-amr, https://github.com/Shyamili09/ARGs-Antibiogram-comparison and https://doi.org/10.5281/zenodo.19000549[68].

Authors' contribution

KBT, JJ and DTS conceived and designed the study. BB & PG clinically examined the patients. LL performed antimicrobial susceptibility testing and DNA extraction. RB and SA carried out library preparation and sequencing. VSK, ARP, AK and RJM conducted the bioinformatics analysis. AP performed comparative genome analysis. VSK prepared the first draft of the manuscript, which was reviewed and edited by KBT, JJ, DTS, PG, BB and VKN. ArP was responsible for project management. All authors read and approved of the final manuscript.

Competing interests

The authors declare no competing interests.

Acknowledgements

The study was made possible by funding from the Rockefeller Foundation (Grant 2021 HTH 018). We acknowledge Prof. L S Shashidhara for his guidance. Hyderabad Eye Research Foundation (HERF) for facilitating project execution. The HPC facility of CCMB is acknowledged for providing computational resources for data analysis.

References:

1. Naghavi, M. et al. Global burden of bacterial antimicrobial resistance 1990–2021: a systematic analysis with forecasts to 2050. The Lancet 404, 1199–1226 (2024).
2. Murray, C. J. L. et al. Global burden of bacterial antimicrobial resistance in 2019: a systematic analysis. The Lancet 399, 629–655 (2022).

3. Ikuta, K. S. et al. Global mortality associated with 33 bacterial pathogens in 2019: a systematic analysis for the Global Burden of Disease Study 2019. The Lancet 400, 2221–2248 (2022).
4. Snyder, R. W. & Glasser, D. B. Antibiotic therapy for ocular infection. West. J. Med. 161, 579–584 (1994).
5. Ho, C. S. et al. Antimicrobial resistance: a concise update. Lancet Microbe 6, (2025).
6. Asbell, P. A. et al. Antibiotic Resistance Among Ocular Pathogens in the United States: Five-Year Results From the Antibiotic Resistance Monitoring in Ocular Microorganisms (ARMOR) Surveillance Study. JAMA Ophthalmol. 133, 1445–1454 (2015).
7. Asbell, P. A., Sanfilippo, C. M. & DeCory, H. H. Antibiotic resistance of bacterial pathogens isolated from the conjunctiva in the Antibiotic Resistance Monitoring in Ocular Microorganisms (ARMOR) surveillance study (2009-2021). Diagn. Microbiol. Infect. Dis. 108, 116069 (2024).
8. Miranda, S. W., André, C., Bispo, P. J. M. & Gilmore, M. S. Whole Genome Analysis of Ocular Pseudomonas aeruginosa Isolates Reveals Genetic Diversity. Invest. Ophthalmol. Vis. Sci. 66, 58 (2025).
9. Kandasamy, K. et al. Comparative genomics of ocular Pseudomonas aeruginosa strains from keratitis patients with different clinical outcomes. Genomics 112, 4769–4776 (2020).
10. Cabrera-Aguas, M., Chidi-Egboka, N., Kandel, H. & Watson, S. L. Antimicrobial resistance in ocular infection: A review. Clin. Experiment. Ophthalmol. 52, 258–275 (2024).
11. Das, A. V. & Joseph, J. The landscape of bacterial antibiotic susceptibility in a multi-tier ophthalmology network in India: an electronic medical record driven analytics report. J. Med. Microbiol. 71, (2022).
12. Ting, D. S. J., Ho, C. S., Deshmukh, R., Said, D. G. & Dua, H. S. Infectious keratitis: an update on epidemiology, causative microorganisms, risk factors, and antimicrobial resistance. Eye Lond. Engl. 35, 1084–1101 (2021).

13. Gandepalli, L. et al. Microbiological profile and antibiotic resistance trends of preoperative conjunctival swabs: An 8-year retrospective analysis from a North Indian tertiary care ophthalmic center. Indian J Ophthalmol 74, 98–103 (2026).
14. Xu, Y. et al. Etiological characteristics of 3,691 cases of microbial keratitis: an 8-year longitudinal study. Microbiology Spectrum 13, e02630-24 (2025).
15. Ceylan, A. et al. Microbiological profile and antibiotic susceptibility results in corneal samples: Sharing 4-year data. EUROPEAN EYE RESEARCH 5, 138–144 (2025).
16. Drago, L. et al. Antibiotic Resistance Profiles in Eye Infections: A Local Concern with a Retrospective Focus on a Large Hospital in Northern Italy. Microorganisms 12, 984 (2024).
17. Asbell, P. A., Sanfilippo, C. M., Sahm, D. F. & DeCory, H. H. Trends in Antibiotic Resistance Among Ocular Microorganisms in the United States From 2009 to 2018. JAMA Ophthalmol 138, 439–450 (2020).
18. Wheeler, N. E. et al. Innovations in genomic antimicrobial resistance surveillance. Lancet Microbe 4, e1063–e1070 (2023).
19. Okeke, I. N. et al. The scope of the antimicrobial resistance challenge. Lancet Lond. Engl. 403, 2426–2438 (2024).
20. Jesudason, T. WHO publishes updated list of bacterial priority pathogens. Lancet Microbe 5, 100940 (2024).
21. Baker, K. S. et al. Evidence review and recommendations for the implementation of genomics for antimicrobial resistance surveillance: reports from an international expert group. Lancet Microbe 4, e1035–e1039 (2023).
22. Jauneikaite, E. et al. Genomics for antimicrobial resistance surveillance to support infection prevention and control in health-care facilities. Lancet Microbe 4, e1040–e1046 (2023).
23. Djordjevic, S. P. et al. Genomic surveillance for antimicrobial resistance - a One Health perspective. Nat. Rev. Genet. 25, 142–157 (2024).

24. Yang, W., Chen, T., Zhou, Q. & Xu, J. Resistance to linezolid in Staphylococcus aureus by mutation, modification, and acquisition of genes. J. Antibiot. (Tokyo) 78, 4–13 (2025).
25. Smith, C. A. & Thomas, C. M. Deletion mapping of kil and kor functions in the trfA and trfB regions of broad host range plasmid RK2. Mol. Gen. Genet. MGG 190, 245–254 (1983).
26. McLean, T. C. et al. KorB switching from DNA-sliding clamp to repressor mediates long-range gene silencing in a multi-drug resistance plasmid. Nat. Microbiol. 10, 448–467 (2025).
27. Kostelidou, K. & Thomas, C. M. The hierarchy of KorB binding at its 12 binding sites on the broad-host-range plasmid RK2 and modulation of this binding by IncC1 protein. J. Mol. Biol. 295, 411–422 (2000).
28. Johnson, W.L., et al. Genomics of Staphylococcus aureus ocular isolates. *PLoS One*, *16*(5), p.e0250975 (2021).
29. André, C., et al.. Microbiology of eye infections at the Massachusetts Eye and Ear: an 8-year retrospective review combined with genomic epidemiology. *American journal of ophthalmology*, *255*, pp.43-56 (2023).
30. Yuan, H. et al. The Global Antimicrobial Resistance Trends of Staphylococcus aureus and Influencing Factors. Microbiol. Res. 16, 118 (2025).
31. Zhao, H. et al. Phenotypic and genomic analysis of the hypervirulent ST22 methicillin-resistant Staphylococcus aureus in China. mSystems 8, e0124222 (2023).
32. Yamaguchi, T. et al. Evolutionary dynamics of the novel ST22-PT methicillin-resistant Staphylococcus aureus clone co-harbouring Panton–Valentine leucocidin and duplicated toxic shock syndrome toxin 1 genes. Clin. Microbiol. Infect. 30, 779–786 (2024).
33. Guo, Y. et al. Whole-genome sequencing reveals resistance mechanisms and molecular epidemiology of carbapenem-resistant Pseudomonas aeruginosa bloodstream infections. BMC Microbiol. 25, 679 (2025).
34. Li, J. et al. Molecular characterization of extensively drug-resistant hypervirulent

Pseudomonas aeruginosa isolates in China. Ann. Clin. Microbiol. Antimicrob. 23, 13 (2024).

35. Li, Z. et al. Molecular genetic analysis of an XDR Pseudomonas aeruginosa ST664 clone carrying multiple conjugal plasmids. J. Antimicrob. Chemother. 75, 1443–1452 (2020).
36. Bakthavatchalam, Y. D., Anandan, S. & Veeraraghavan, B. Laboratory detection and clinical implication of oxacillinase-48 like carbapenemase: the hidden threat. *J. Glob. Infect. Dis.* **8**, 41–50 (2016).
37. Shaidullina, E. R. et al. Genomic analysis of the international high-risk clonal lineage Klebsiella pneumoniae sequence type 395. Genome Med. 15, 9 (2023).
38. Rolbiecki, D. et al. Genomic and metagenomic analysis reveals shared resistance genes and mobile genetic elements in E. coli and Klebsiella spp. isolated from hospital patients and hospital wastewater at intra- and inter-genus level. Int. J. Hyg. Environ. Health 261, 114423 (2024).
39. Liu, C. et al. Emergence and Inter- and Intrahost Evolution of Pandrug-Resistant Klebsiella pneumoniae Coharboring tmexCD1-toprJ1, blaNDM-1, and blaKPC-2. Microbiol. Spectr. 11, e02786-22 (2023).
40. Zhou, H. et al. Genomic census of invasive nontyphoidal Salmonella infections reveals global and local human-to-human transmission. Nat. Med. 31, 2325–2334 (2025).
41. Yang, W., et al. Resistance to linezolid in Staphylococcus aureus by mutation, modification, and acquisition of genes. J. Antibiot. (Tokyo) 78, 4–13 (2025).
42. De Coster, W. & Rademakers, R. NanoPack2: population-scale evaluation of long-read sequencing data. Bioinformatics 39, btad311 (2023).
43. Wood, D. E., Lu, J. & Langmead, B. Improved metagenomic analysis with Kraken 2. Genome Biol. 20, 257 (2019).
44. Koren, S. et al. Canu: scalable and accurate long-read assembly via adaptive k-mer weighting and repeat separation. Genome Res. 27, 722–736 (2017).

45. Chen, Y., Zhang, Y., Wang, A. Y., Gao, M. & Chong, Z. Accurate long-read de novo assembly evaluation with Inspector. Genome Biol. 22, 312 (2021).
46. Parks, D. H., Imelfort, M., Skennerton, C. T., Hugenholtz, P. & Tyson, G. W. CheckM: assessing the quality of microbial genomes recovered from isolates, single cells, and metagenomes. Genome Res. 25, 1043–1055 (2015).
47. Jain, C., Rodriguez-R, L. M., Phillippy, A. M., Konstantinidis, K. T. & Aluru, S. High throughput ANI analysis of 90K prokaryotic genomes reveals clear species boundaries. Nat. Commun. 9, 5114 (2018).
48. Jolley, K. A., Bray, J. E. & Maiden, M. C. J. Open-access bacterial population genomics: BIGSdb software, the PubMLST.org website and their applications. Wellcome Open Res. 3, 124 (2018).
49. Alcock, B. P. et al. CARD 2023: expanded curation, support for machine learning, and resistome prediction at the Comprehensive Antibiotic Resistance Database. Nucleic Acids Res. 51, D690–D699 (2023).
50. Li, H. Minimap2: pairwise alignment for nucleotide sequences. Bioinformatics 34, 3094–3100 (2018).
51. Li, H. et al. The Sequence Alignment/Map format and SAMtools. Bioinformatics 25, 2078–2079 (2009).
52. Quinlan, A. R. & Hall, I. M. BEDTools: a flexible suite of utilities for comparing genomic features. Bioinformatics 26, 841–842 (2010).
53. Camargo, A. P. et al. Identification of mobile genetic elements with geNomad. Nat. Biotechnol. 42, 1303–1312 (2024).
54. Carattoli, A. & Hasman, H. PlasmidFinder and In Silico pMLST: Identification and Typing of Plasmid Replicons in Whole-Genome Sequencing (WGS). Methods Mol. Biol. Clifton NJ 2075, 285–294 (2020).
55. McMurdie, P. J. & Holmes, S. phyloseq: an R package for reproducible interactive analysis

and graphics of microbiome census data. PloS One 8, e61217 (2013).

56. Jacomy, M., Venturini, T., Heymann, S. & Bastian, M. ForceAtlas2, a continuous graph layout algorithm for handy network visualization designed for the Gephi software. PloS One 9, e98679 (2014).
57. Grant, J. R. et al. Proksee: in-depth characterization and visualization of bacterial genomes. Nucleic Acids Res. 51, W484–W492 (2023).
58. Shetty, S. A. & Lahti, L. Microbiome data science. J. Biosci. 44, 115 (2019).
59. Seemann, T. Prokka: rapid prokaryotic genome annotation. Bioinformatics 30, 2068–2069 (2014).
60. Page, A. J. et al. Roary: rapid large-scale prokaryote pan genome analysis. Bioinforma. Oxf. Engl. 31, 3691–3693 (2015).
61. Stamatakis, A. RAxML version 8: a tool for phylogenetic analysis and post-analysis of large phylogenies. Bioinforma. Oxf. Engl. 30, 1312–1313 (2014).
62. Letunic, I. & Bork, P. Interactive Tree Of Life (iTOL) v4: recent updates and new developments. Nucleic Acids Res. 47, W256–W259 (2019).
63. Kaya, H. et al. SCCmecFinder, a Web-Based Tool for Typing of Staphylococcal Cassette Chromosome mec in Staphylococcus aureus Using Whole-Genome Sequence Data. mSphere 3, e00612-17 (2018).
64. Kumar, S., Stecher, G., Li, M., Knyaz, C. & Tamura, K. MEGA X: Molecular Evolutionary Genetics Analysis across Computing Platforms. Mol. Biol. Evol. 35, 1547–1549 (2018).
65. Le, D. Q. et al. AMRomics: a scalable workflow to analyze large microbial genome collections. BMC Genomics 25, 709 (2024).
66. Schliep, K. P. phangorn: phylogenetic analysis in R. Bioinforma. Oxf. Engl. 27, 592–593 (2011).
67. Tallapaka, K. Genomic Insights into Antimicrobial Resistance in Ocular Pathogens from India [Data Set]. Zenodo https://doi.org/10.5281/zenodo.18996254

68. Tallapaka, K. Genomic Insights into Antimicrobial Resistance in Ocular Pathogens from India. Zenodo https://doi.org/10.5281/zenodo.19000549

Figure Legends:

Figure 1. Sample collection, processing, and distribution of bacterial isolates in ocular infections.
A. Anatomical sites of the eye from which isolates yielding 291 high-quality genome assemblies in this study were obtained. (Created in BioRender. punde, A. (2026) https://BioRender.com/zzqgquk) Numbers in parentheses indicate the percentage and count of isolates collected from each site. Species-wise distribution of sequenced isolates across different anatomical layers of the eye is represented as a stacked bar plot. **B.** Computational workflow in the study.

Figure 2. Genotype–phenotype concordance of antimicrobial resistance across major ocular bacterial pathogens.
Concordance between genomic predictions of antimicrobial resistance and phenotypic susceptibility profiles: **A.** *Staphylococcus aureus* (60); **B.** *Staphylococcus epidermidis* (34); **C.** *Pseudomonas aeruginosa* (62) and **D.** *Klebsiella pneumoniae* (11). Isolates were classified into eight categories of genotype-phenotype concordance based on the presence or absence of known ARGs and corresponding antimicrobial susceptibility testing (AST) results (resistant/sensitive/SDD/not-tested). Horizontal bars represent the percentage of isolates in each concordance category for antibiotics. Antibiotics are grouped and ordered by antibiotic classes.

Figure 3. Distribution and abundance of antimicrobial resistance genes across Gram-positive and Gram-negative ocular bacterial isolates.
Circular visualization depicting the abundance and diversity of antimicrobial resistance genes (ARGs) identified in **A.** gram-positive bacterial isolates (138) and **B.** gram-negative bacterial isolates (153). The outer ring represents individual bacterial isolates, color-coded by species as indicated in the legend. Inner arcs represent ARGs detected in each isolate, with arc thickness corresponding to gene abundance quantified as fragments per kilobase of transcript per million mapped reads.

Figure 4. Sequence types and genotype-phenotype associations of antimicrobial resistance in A. *Staphylococcus aureus* and B. *Staphylococcus epidermidis* isolates.

The leftmost columns display antimicrobial susceptibility testing (AST) results for major antibiotics, with filled circles indicating resistance (red) or sensitivity (green) status. Empty circles indicate non availability of AST results. Adjacent heatmaps display the abundance (percentage of total ARGs in the isolate) of corresponding ARGs detected in each isolate, with color intensity (shades of blue). ARGs are organized into columns by antibiotic class as indicated by the color-coded header. The rightmost column displays the sequence type (ST) assignment for each isolate based on multilocus sequence typing (MLST). Isolates carrying only *gyrA* (S84L) and *parC* (S80F or S80Y) Quinolone resistance-determining regions (QRDR) mutations were included in this analysis.

Figure 5. Sequence type distribution and genotype-phenotype associations of antimicrobial resistance in A. *Pseudomonas aeruginosa* and B. *Klebsiella pneumoniae* isolates.

The leftmost columns display antimicrobial susceptibility testing (AST) results for major antibiotics, with filled circles indicating resistance (red) or sensitivity (green) status. Empty circles indicate non availability of AST results. Adjacent heatmaps display the abundance (percentage of total ARGs in the isolate) of corresponding ARGs detected in each isolate, with color intensity (shades of blue). ARGs are organized into columns by antibiotic class as indicated by the color-coded header. The rightmost column displays the sequence type (ST) assignment for each isolate based on multilocus sequence typing (MLST). Isolates carrying Quinolone resistance-determining regions (QRDR) mutations in the genes *gyrA* T83I or *parE* A473V were only included in this analysis.

Figure 6. Plasmid-encoded antimicrobial resistance genes in gram-negative ocular pathogens.

A. Network analysis depicting plasmids and their associated antimicrobial resistance genes (ARGs) in gram-negative bacterial isolates. Nodes represent plasmids or ARGs, with plasmids shown as pentagons (conjugative plasmids containing mobility genes) or triangles (non-conjugative plasmids lacking genes). ARGs are represented as circles, color-coded by antibiotic resistance class (legend shown). Edges connect plasmids to their ARGs. Node size is proportional to the degree of connectivity. **B.** Circos plots illustrating sequence similarity across plasmids from *Escherichia coli* and *Klebsiella pneumoniae* isolates. **C.** Genomic architecture of plasmids harboring the bla_{OXA-1} β-lactamase gene in multidrug-resistant (MDR) *K. pneumoniae* (top) and *E. coli* (bottom) isolates. Linear plasmid maps show the position and orientation of key genetic elements including ARGs and (mobile genetic elements) MGEs.

Figure 7. Genomic architecture of plasmids in a high-risk multidrug-resistant *Klebsiella pneumoniae* isolate.

Linear plasmid maps showing the genetic organization and context of carbapenemase genes in a high-risk *K. pneumoniae* (ST395-1LV) isolate carrying multiple resistance plasmids. **A.** Plasmid contig harboring bla_{NDM-1}. **B.** Plasmid contig carrying bla_{NDM-5}. **C.** Plasmid contig containing $bla_{oxa-232}$

Figure 8. Phylogeographic analysis and molecular characterization of linezolid resistance in a vancomycin-resistant *Staphylococcus aureus* (VRSA) isolate.

A. Maximum-likelihood phylogenetic tree constructed from core-genome single nucleotide polymorphism (SNP) alignment of 245 *S. aureus* genomes, comprising 60 isolates from this study and 185 publicly available reference genomes. The tree reveals the evolutionary relationships and geographic distribution of *S. aureus* lineages. The innermost ring indicates the geographic origin of isolates. The outermost ring indicates sequence types. In-house isolates color-coded: red text indicates isolates belonging to previously characterized STs, while blue text denotes previously unreported STs identified in this study. The phylogenetic analysis positions the ST9578

isolate, revealing its genetic distinctiveness and evolutionary origin. **B.** Multiple sequence alignment of the 23S rRNA gene from 12 representative S. aureus isolates aligned against all six 23S rRNA gene copies from the ST9578 (OI209). A unique G1549A mutation associated with linezolid resistance was consistently observed in all 6 copies of 23S rRNA from the ST9578 genome. The consensus sequence is marked with * for 100% identity.

Editor Summary

Genomic surveillance identifies emerging XDR strains and putative AMR mechanisms in isolates from ocular infections in India.

Peer Review Information

Communications Biology thanks the anonymous reviewer(s) for their contribution to the peer review of this work. Primary Handling Editors: Tobias Goris and George Inglis. A peer review file is available.

A Sample collection :

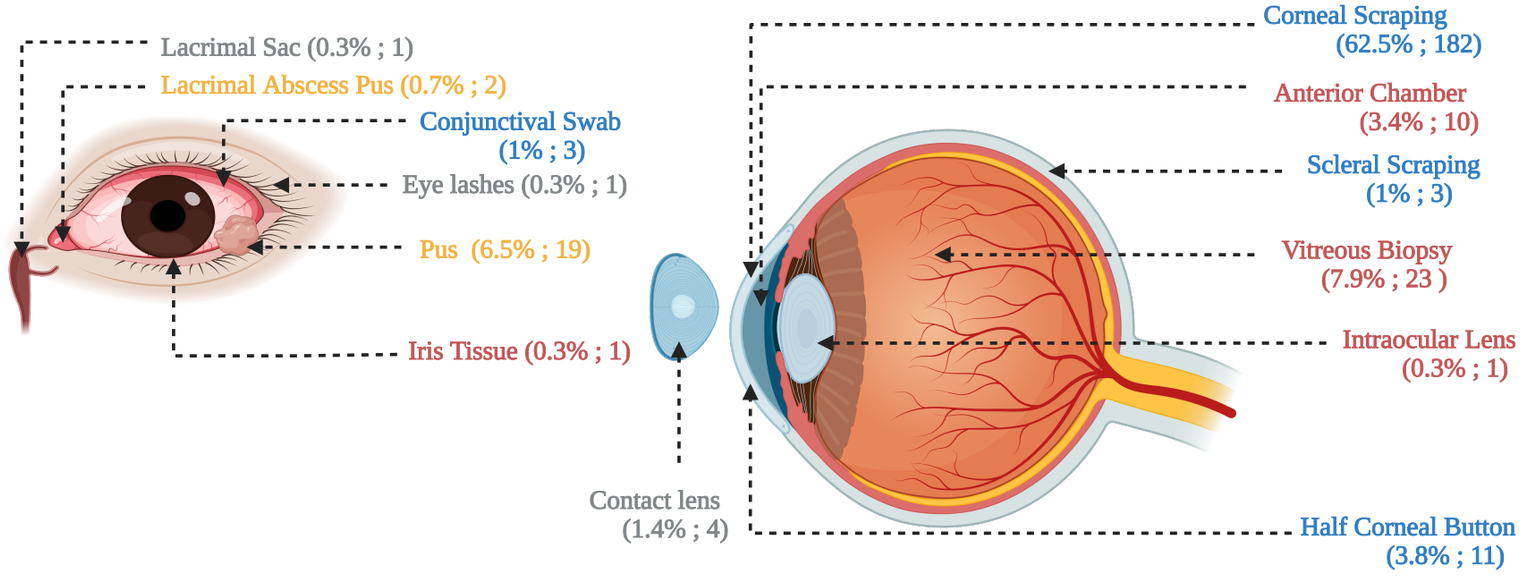

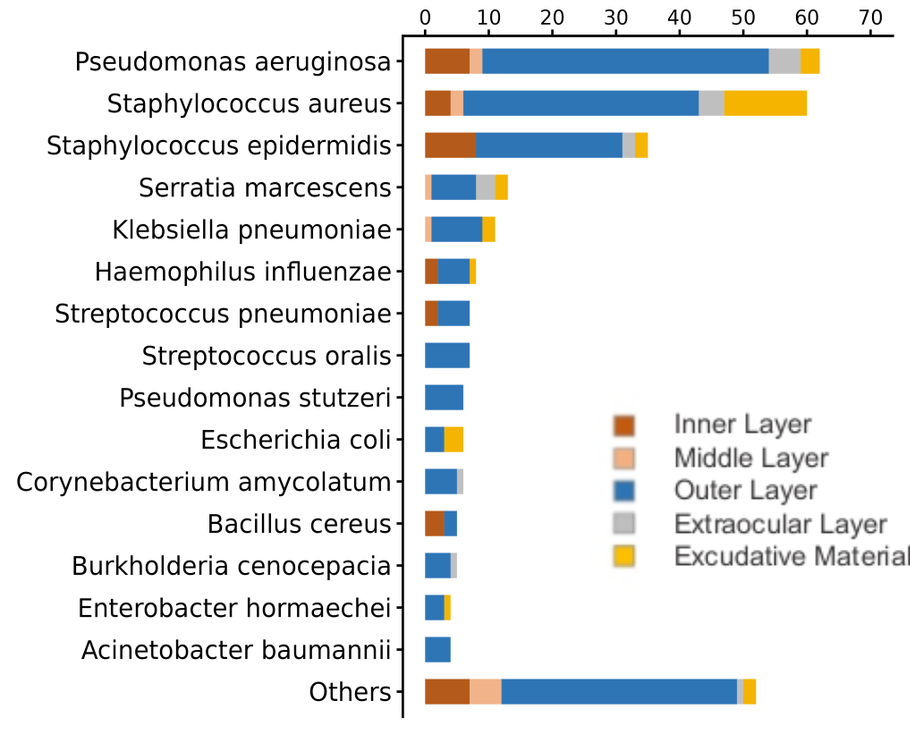

B Bioinformatics Pipeline :

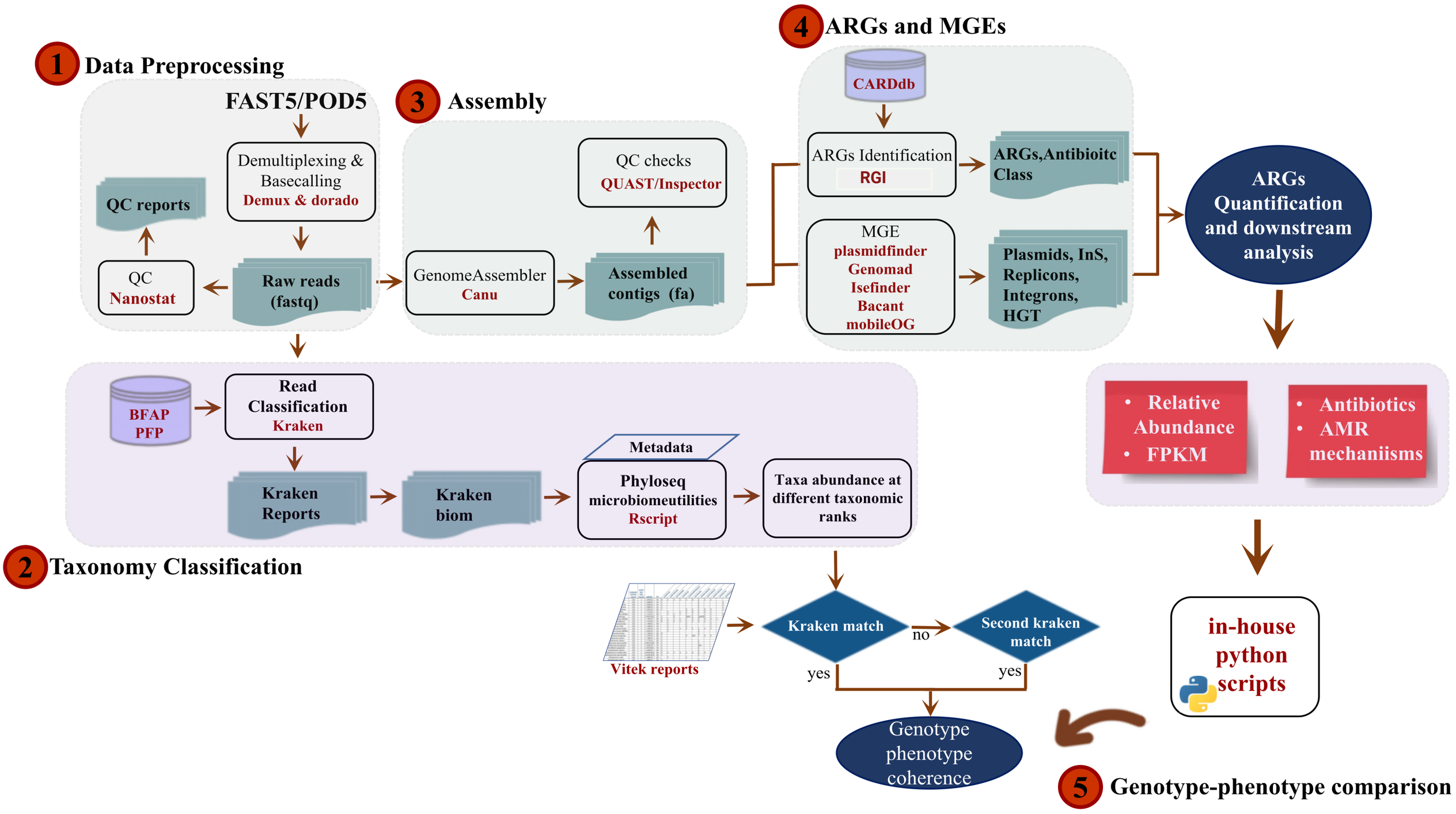

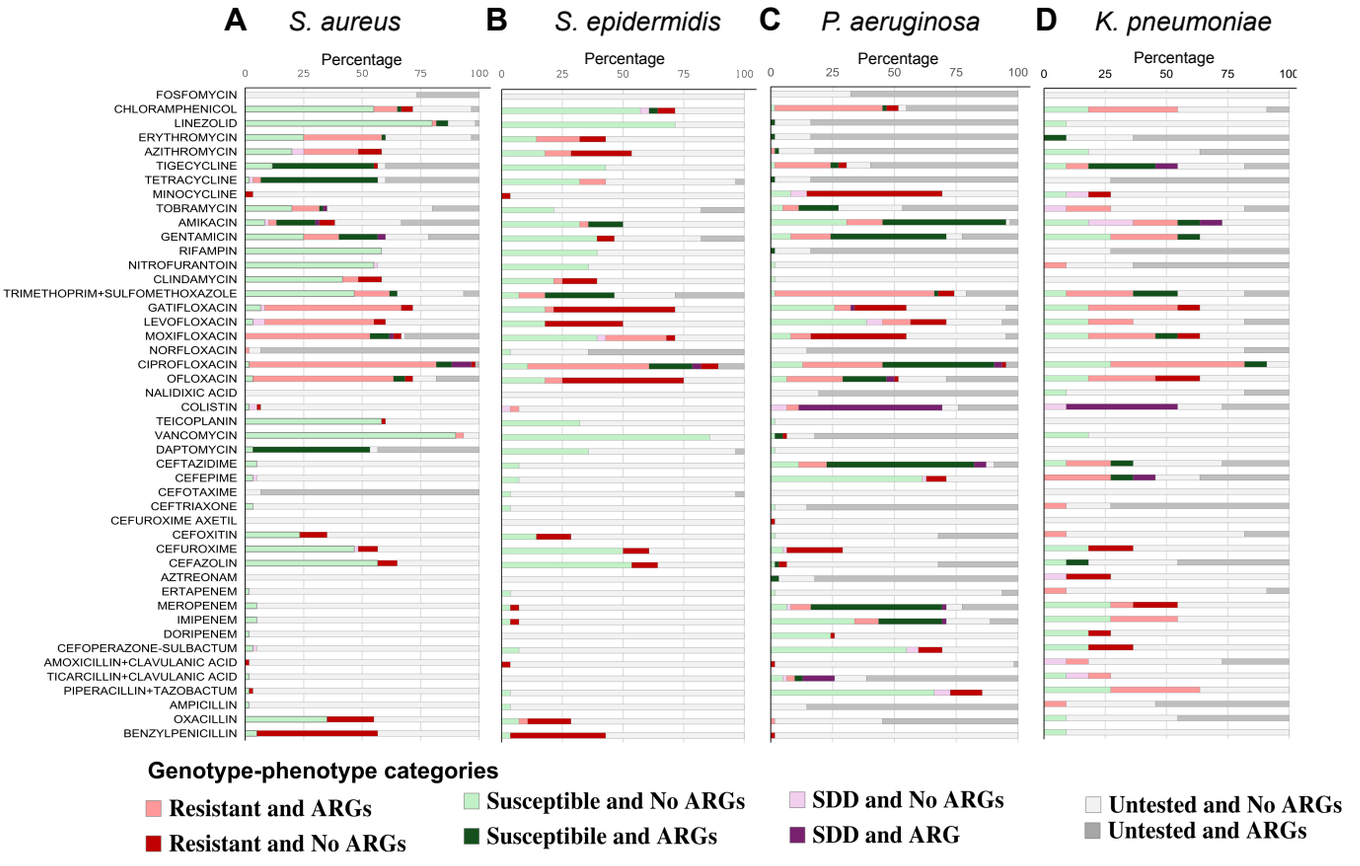
A S. aureus
B S. epidermidis
C P. aeruginosa
D K. pneumoniae
Percentage
0 25 50 75 100
FOSFOMYCIN
CHLORAMPHENICOL
LINEZOLID
ERYTHROMYCIN
AZITHROMYCIN
TIGECYCLINE
TETRACYCLINE
MINOCYCLINE
TOBRAMYCIN
AMIKACIN
GENTAMICIN
RIFAMPIN
NITROFURANTOIN
CLINDAMYCIN
TRIMETHOPRIM+SULFOMETHOXAZOLE
GATIFLOXACIN
LEVOFLOXACIN
MOXIFLOXACIN
NORFLOXACIN
CIPROFLOXACIN
OFLOXACIN
NALIDIXIC ACID
COLISTIN
TEICOPLANIN
VANCOMYCIN
DAPTOMYCIN
CEFTAZIDIME
CEFEPIME
CEFOTAXIME
CEFTRIAXONE
CEFUROXIME AXETIL
CEFOXITIN
CEFUROXIME
CEFAZOLIN
AZTREONAM
ERTAPENEM
MEROPENEM
IMIPENEM
DORIPENEM
CEFOPERAZONE-SULBACTUM
AMOXICILLIN+CLAVULANIC ACID
TICARCILLIN+CLAVULANIC ACID
PIPERACILLIN+TAZOBACTUM
AMPICILLIN
OXACILLIN
BENZYLPENICILLIN
Genotype-phenotype categories
Resistant and ARGs
Resistant and No ARGs
Susceptible and No ARGs
Susceptibile and ARGs
SDD and No ARGs
SDD and ARG
Untested and No ARGs
Untested and ARGs

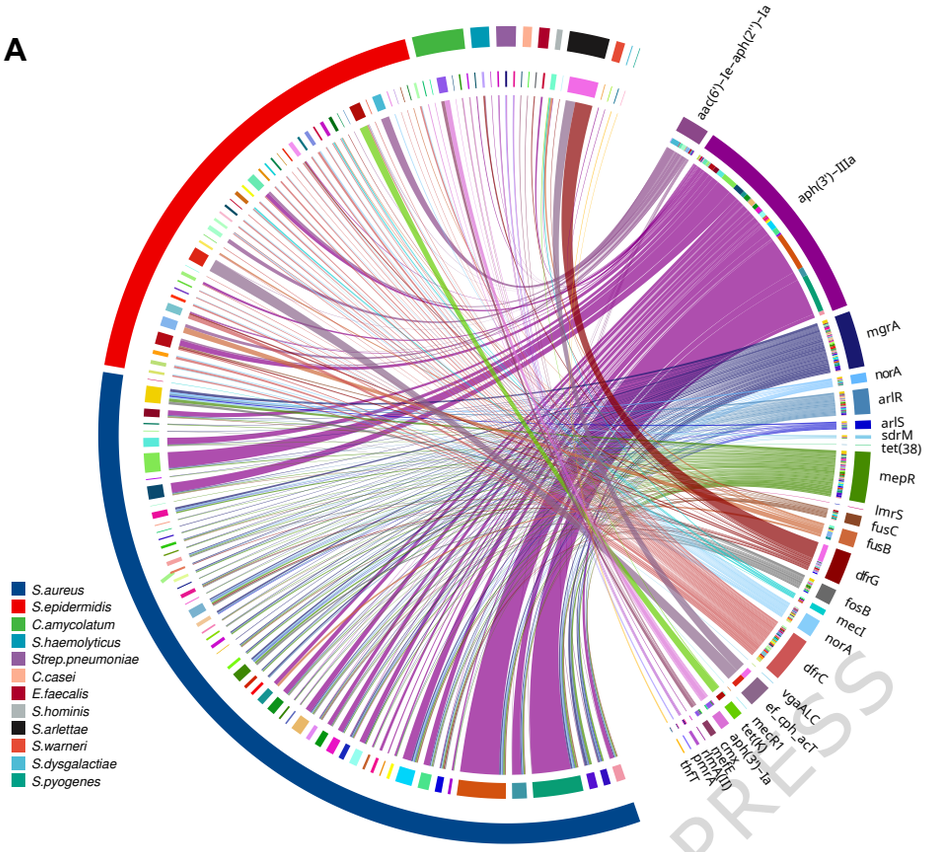

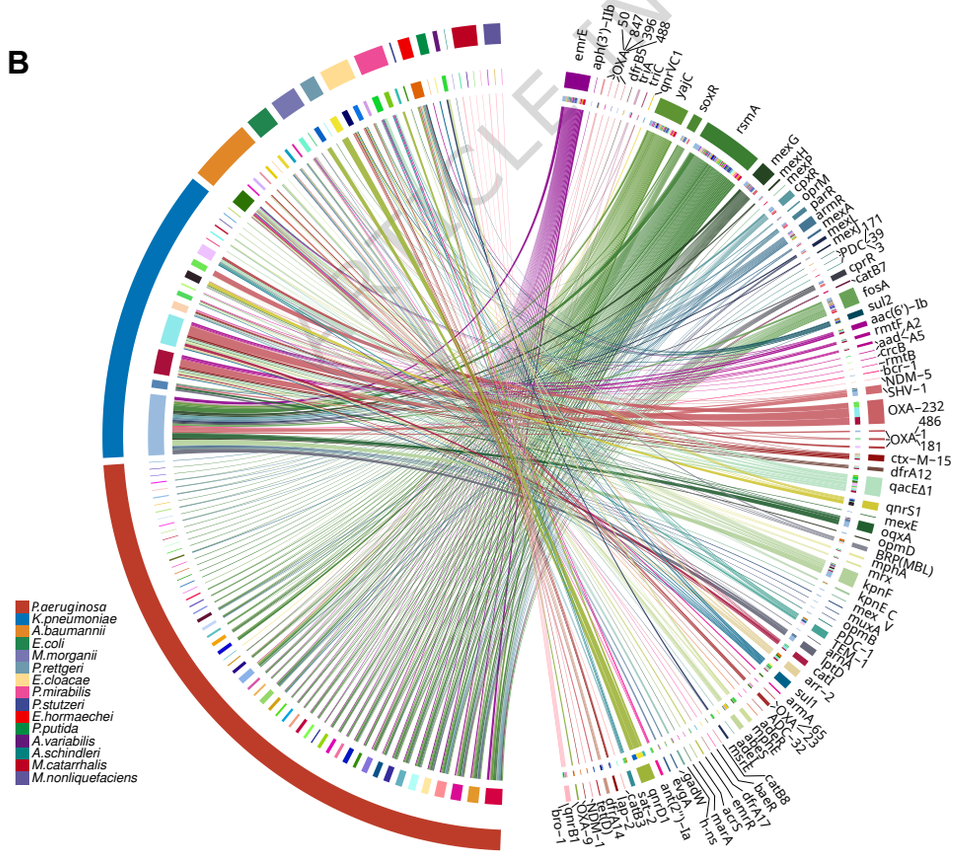

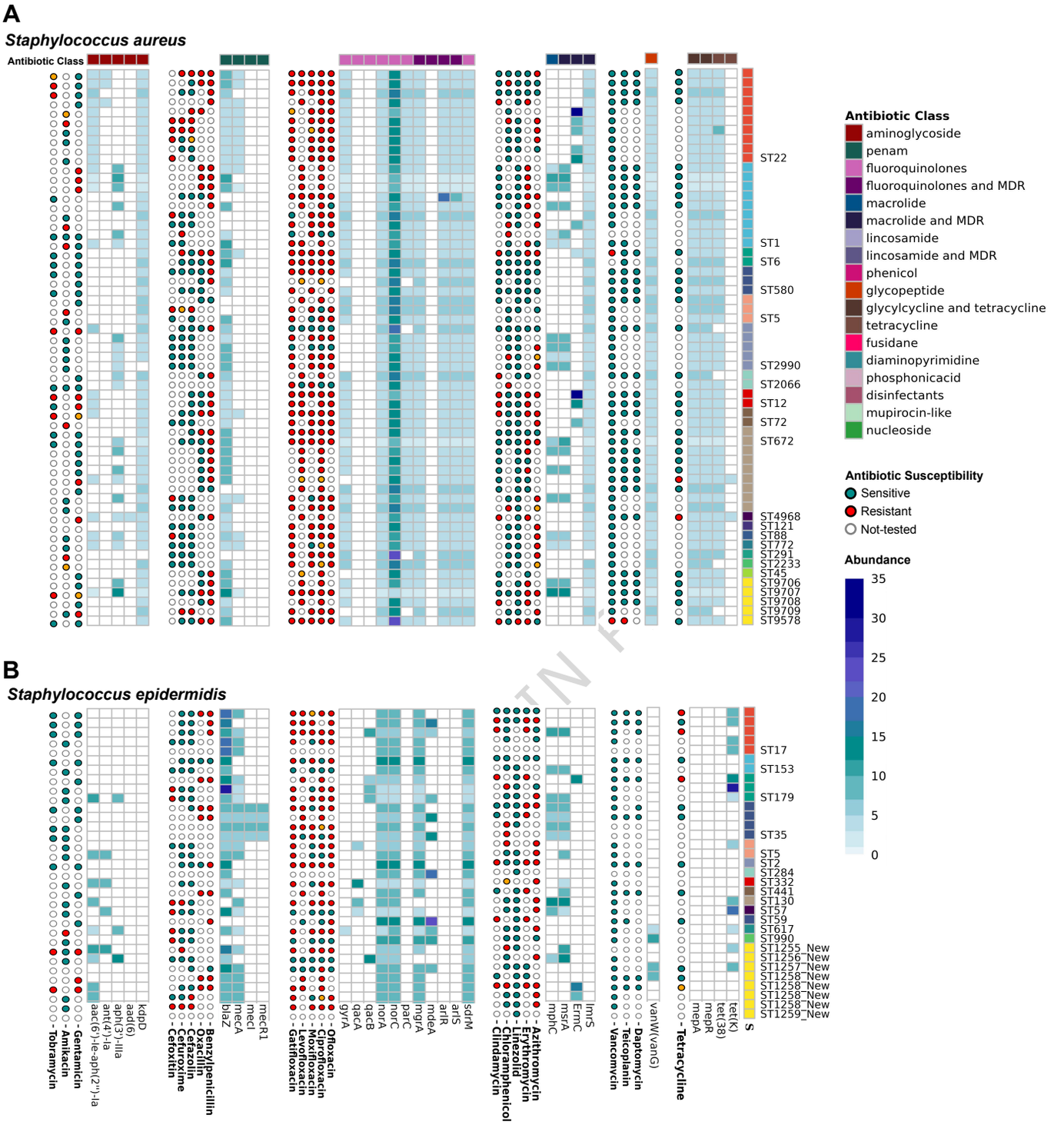

A

Pseudomonas aeruginosa

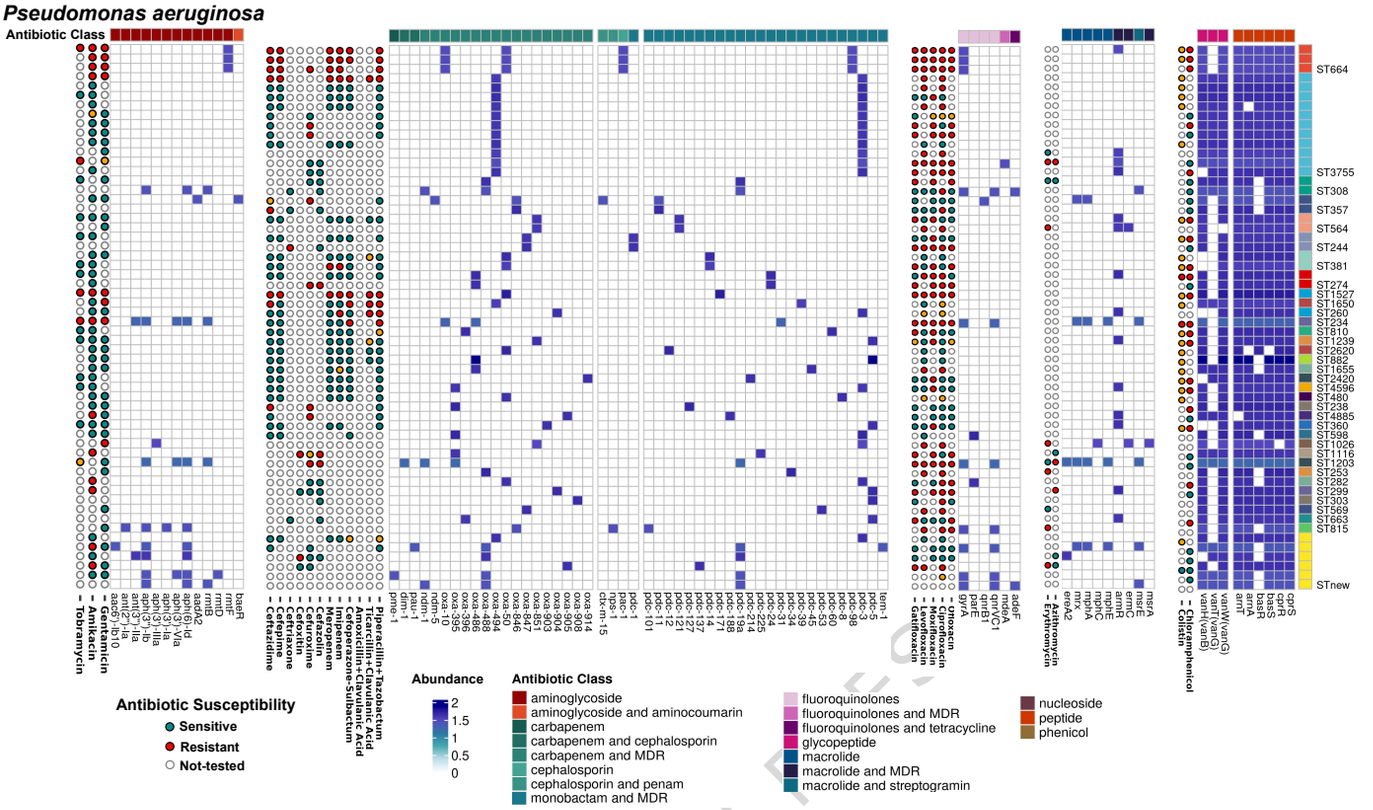

B

Klebsiella pneumoniae

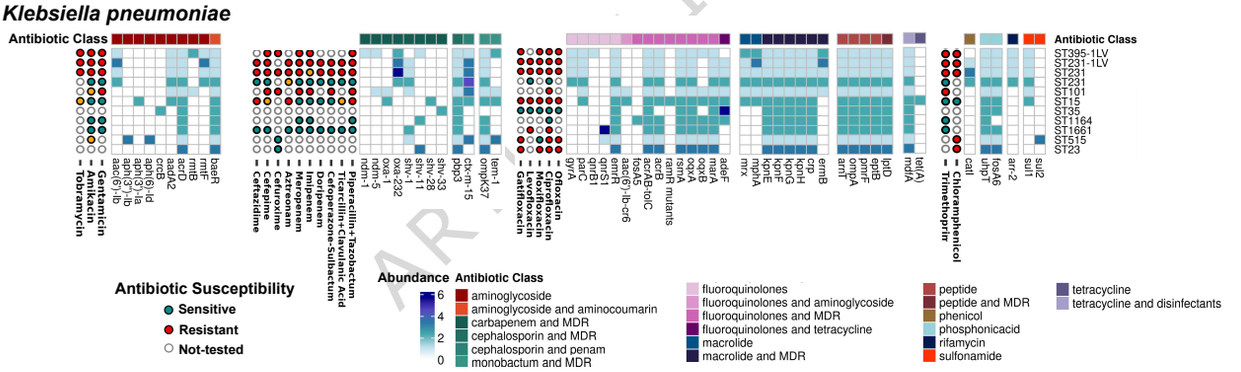

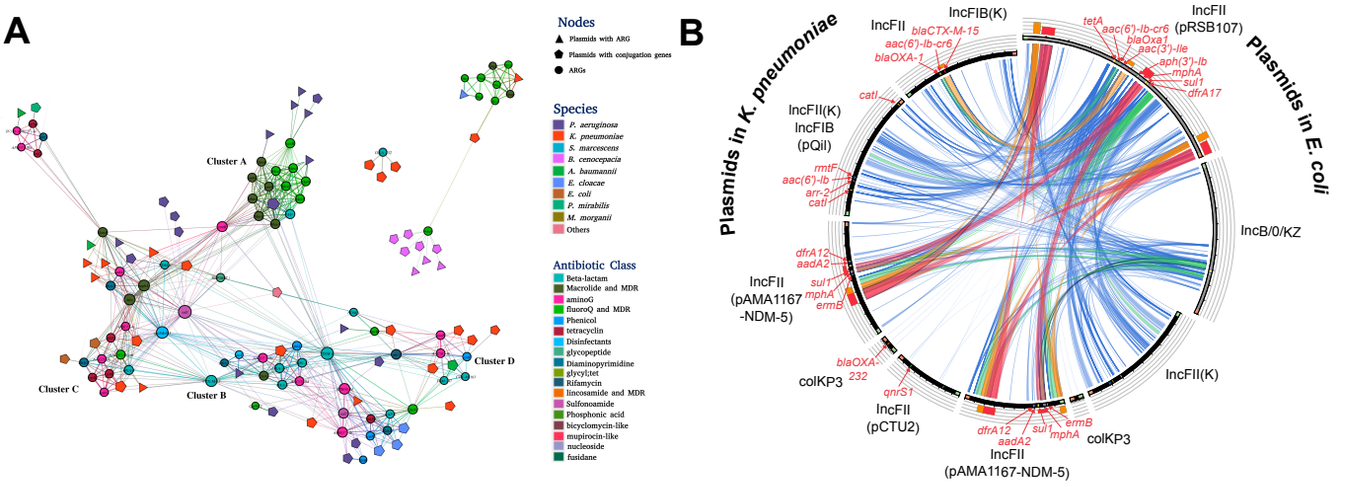

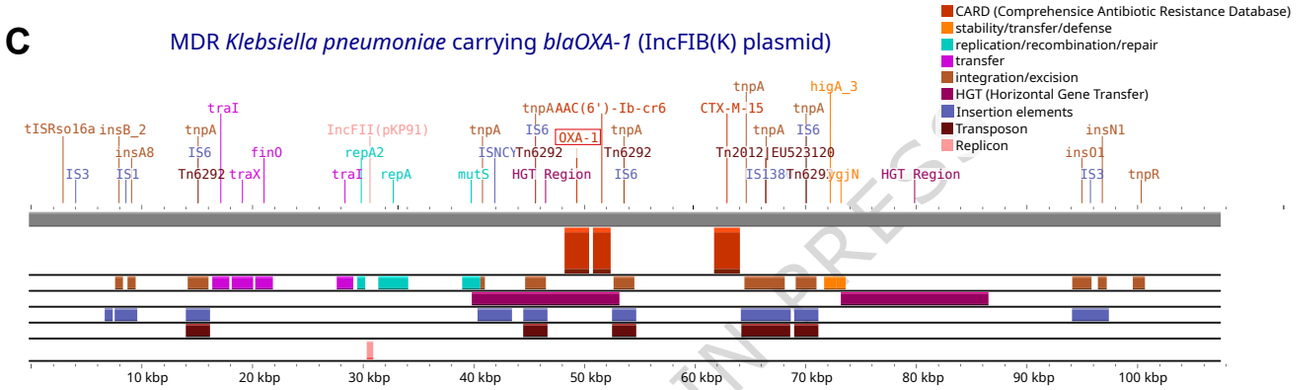

A

MDR *Klebsiella pneumonia* carrying *blaNDM-1* (IncFII(K) plasmid)

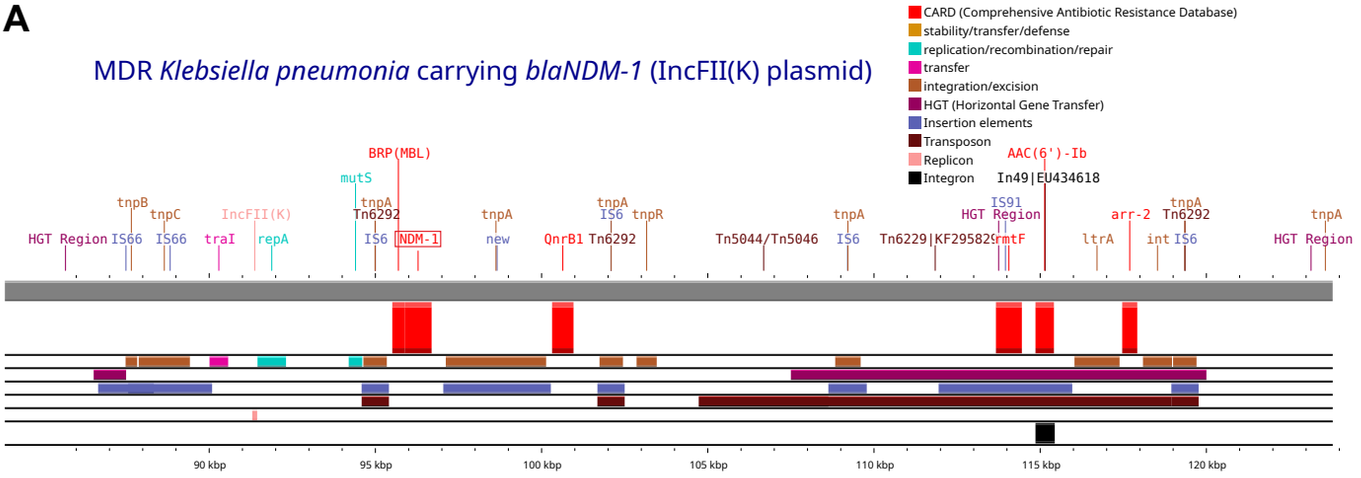

B

MDR *Klebsiella pneumonia* carrying *blaNDM-5* (IncFII plasmid)

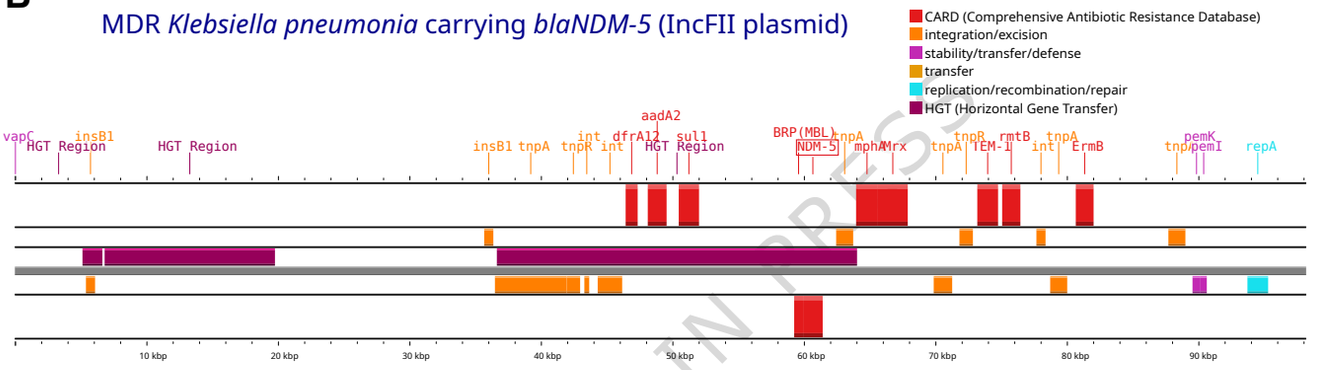

C

MDR *Klebsiella pneumonia* carrying *blaOXA-232* (ColKP3 plasmid)

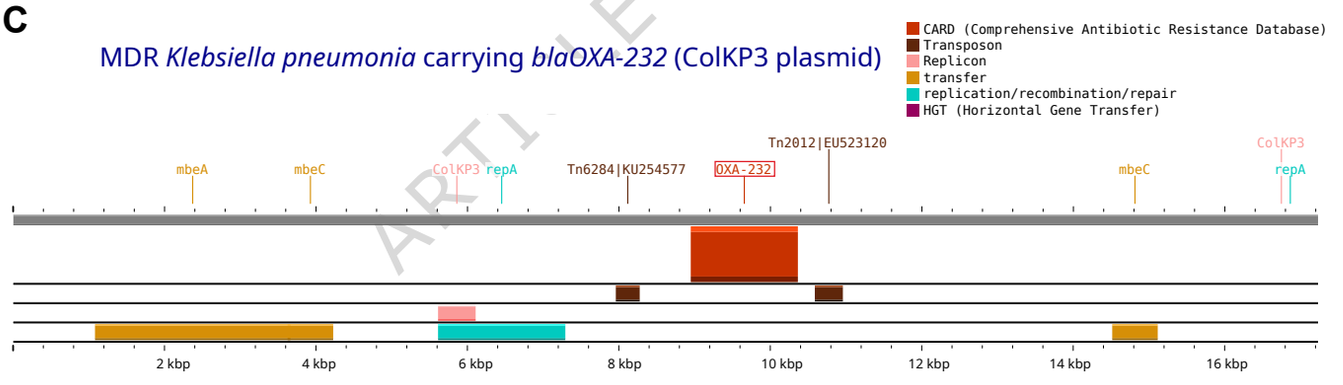

A

B

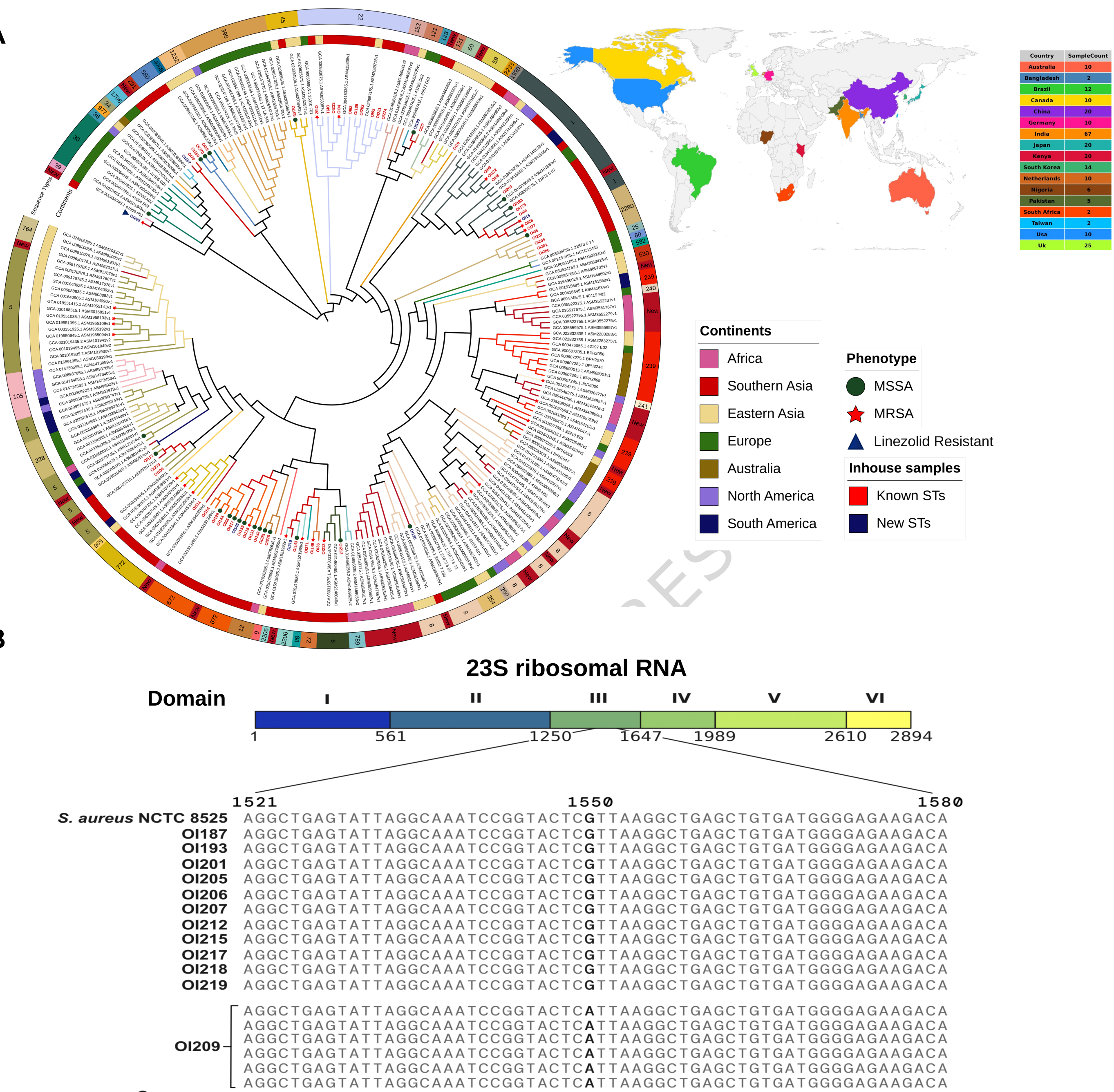
Country | SampleCount
Australia 10
Bangladesh 2
Brazil 12
Canada 10
China 20
Germany 10
India 67
Japan 20
Kenya 20
South Korea 14
Netherlands 10
Nigeria 6
Pakistan 5
South Africa 2
Taiwan 2
Usa 10
Uk 25
Sequence Types
Continents
Continents
Africa
Southern Asia
Eastern Asia
Europe
Australia
North America
South America
Phenotype
MSSA
MRSA
Linezolid Resistant
Inhouse samples
Known STs
New STs
23S ribosomal RNA
Domain
I
II
III
IV
V
VI
1
561
1250
1647
1989
2610
2894
1521
1550
1580
S. aureus NCTC 8525 AGGCTGAGTATTAGGCAAATCCGGTACTCGTTAAGGCTGAGCTGTGATGGGGAGAAGACA
OI187 AGGCTGAGTATTAGGCAAATCCGGTACTCGTTAAGGCTGAGCTGTGATGGGGAGAAGACA
OI193 AGGCTGAGTATTAGGCAAATCCGGTACTCGTTAAGGCTGAGCTGTGATGGGGAGAAGACA
OI201 AGGCTGAGTATTAGGCAAATCCGGTACTCGTTAAGGCTGAGCTGTGATGGGGAGAAGACA
OI205 AGGCTGAGTATTAGGCAAATCCGGTACTCGTTAAGGCTGAGCTGTGATGGGGAGAAGACA
OI206 AGGCTGAGTATTAGGCAAATCCGGTACTCGTTAAGGCTGAGCTGTGATGGGGAGAAGACA
OI207 AGGCTGAGTATTAGGCAAATCCGGTACTCGTTAAGGCTGAGCTGTGATGGGGAGAAGACA
OI212 AGGCTGAGTATTAGGCAAATCCGGTACTCGTTAAGGCTGAGCTGTGATGGGGAGAAGACA
OI215 AGGCTGAGTATTAGGCAAATCCGGTACTCGTTAAGGCTGAGCTGTGATGGGGAGAAGACA
OI217 AGGCTGAGTATTAGGCAAATCCGGTACTCGTTAAGGCTGAGCTGTGATGGGGAGAAGACA
OI218 AGGCTGAGTATTAGGCAAATCCGGTACTCGTTAAGGCTGAGCTGTGATGGGGAGAAGACA
OI219 AGGCTGAGTATTAGGCAAATCCGGTACTCGTTAAGGCTGAGCTGTGATGGGGAGAAGACA
OI209 AGGCTGAGTATTAGGCAAATCCGGTACTCATTAAGGCTGAGCTGTGATGGGGAGAAGACA
AGGCTGAGTATTAGGCAAATCCGGTACTCATTAAGGCTGAGCTGTGATGGGGAGAAGACA
AGGCTGAGTATTAGGCAAATCCGGTACTCATTAAGGCTGAGCTGTGATGGGGAGAAGACA
AGGCTGAGTATTAGGCAAATCCGGTACTCATTAAGGCTGAGCTGTGATGGGGAGAAGACA
AGGCTGAGTATTAGGCAAATCCGGTACTCATTAAGGCTGAGCTGTGATGGGGAGAAGACA
AGGCTGAGTATTAGGCAAATCCGGTACTCATTAAGGCTGAGCTGTGATGGGGAGAAGACA
Consensus ***************************** ******************************